学位論文

Mechanism of Cortical Microtubule Reorganization in Higher Plant Cells

~ Studies on Tubulin Recycle and Origin of Cortical Microtubules at the M/G_1 interface ~

高等植物細胞における表層微小管再形成機構の解析

～M/G_1 境界期におけるチューブリンのリサイクルと表層微小管の起源に関する研究～

平成 16 年 12 月博士（生命科学）申請

東京大学大学院　新領域創成科学研究科　先端生命科学専攻

米田　新

Mechanism of Cortical Microtubule Reorganization in Higher Plant Cells

~ Studies on Tubulin Recycle and Origin of Cortical Microtubules at the M/G_1 interface ~

Yoneda, Arata

2004

Department of Integrated Bioscience,

Graduate School of Frontier Science,

The University of Tokyo

Acknowlegements

I first wish to express my deepest appreciation to Professor Seiichiro Hasezawa of University of Tokyo for his courteous guidance and continuous encouragement throughout this study. I am also grateful to Dr. Fumi Kumagai of University of Gunma for her kind instructions and constant support.

I thank to Dr. Noriaki Kondo of Teikyo University of Science and Dr. Toshiyuki Nagata of University of Tokyo for their critical advice and useful discussion.

I wish to thank Dr. D. Peter Snustad of University of Minnesota for providing Arabidopsis *TUA3* cDNA and Dr. Yasuo Niwa of University of Shizuoka for the gift of *35S-GFP* (S65T) vector. I wish to express my gratitude to Dr. Hisayoshi Nozaki for his technical advice on the transmission electron microscopy.

Finally, I appreciate all of the members of Lab. of Plant Cell Biology in Totipotency for their help and encouragement.

Contents

Abbreviations

BA : bistheonellide A

BY-2 : A cell line derivered from *Nicotiana tabacum* L. cv. Bright Yellow - 2

BY-GT16 : BY-2 cell line stably expressing GFP-tubulin fusion protein clone 16

CLSM : confocal laser scanning microscopy

CMF : cellulose microfibril

CMT : cortical microtubule

DAPI : 4',6-diamidino-2-phenylindole

FITC : fluorescein-5-isothiocyanate

GFP : green fluorescent protein

MAP : microtubule associated protein

MBD : microtubule binding domain

MBS : *m*-maleimidobenzoyl-*N*-hydroxysuccinimide ester

MF : actin microfilament

MI : mitotic index

MT : microtubule

MTOC : microtubule organizing center

PBS : phosphate-buffered salin (20mM Na phosphate, 150mM NaCl, pH7.0)

PMEG : 50 mM PIPES, 1 mM $MgSO_4$, 5 mM EGTA, 1 % glycerol, pH 6.8

PPB : preprophase band

Summary

In higher plants, microtubules (MTs) play important roles in cell cycle progression and cell morphogenesis. In particular, it is known that cortical MTs (CMTs) regulate the orientation of newly deposited cellulose microfibrils (CMFs), and that the deposition patterns of the CMFs determine the cell shape. The CMTs are decomposed at the G_2/M interface, and then become reorganized at the M/G_1 interface after collapsing telophase phragmoplast. Therefore, the CMT reorganization at the M/G_1 interface is very important phenomenon in plant morphogenesis.

To reveal the MT dynamics, I have established a transgenic BY-2 cell line stably expressing a green fluorescent protein (GFP)-tubulin fusion protein (BY-GT16), and succeeded in investigating the dynamics of tubulin and MTs throughout the cell cycle in the living BY-GT16 cells. The BY-GT16 cells were indistinguishable from the original BY-2 cells in shape and size, and could be highly synchronized by aphidicolin treatment as the original BY-2 cells. The GFP-fluorescence of BY-GT16 represented all the MT structures correctly during the cell cycle, and the MT rearrangements could be continuously observed in the living BY-GT16 under the fluorescence microscopy.

When the BY-GT16 cells were time-sequentially monitored and spatially analyzed by the deconvolution microscopy, the GFP-tubulin was found to accumulate onto the nuclear surface near the cell plate at the final stage of phragmoplast collapse. Subsequently, the GFP-tubulin accumulated again on the nuclear surface opposite the division plane, where the nascent MTs elongated to the cell cortex. When the confocal laser scanning microscopy (CLSM) was used to gain the optical section from the cells, the bright spots were formed where the MTs nucleated from the perinuclear region reached the cell cortex, and the first CMTs rapidly elongated parallel to the cell longitudinal axis from the bright spots towards the distal end of the cells. Around the time when the tips of the parallel CMTs reached the distal end, the formation of transverse CMTs followed on the cell cortex near the division site, and then spread through the whole cell cortex, while the parallel MTs disappeared. The whole processes in the mode of CMT reorganization at the M/G_1 interface were clarified in

detail. In addition, I hypothesize that the tubulin that released from the collapsing phragmoplast was actively transported and recycled as a constituent of the reorganizing CMTs.

When actin microfilaments (MFs) were disrupted by the MF-disrupting agent, bistheonellide A (BA), the tubulin translocation and CMT reorganization did not occur even 3 h after phragmoplast collapse, whereas non-treated cells completed CMT reorganization within 1 h. In the absent of MFs, the tubulin proteins did not show appropriate recruitment but remained at the site where the phragmoplast had existed. Interestingly, some populations of BA-treated cells formed extra-phragmoplast instead of CMTs. Although each extra-phragmoplast showed the mono-layered structures, it functionally formed extra-cell plates. This is the first observation of the formation of multiple cell plates during one nuclear division, and of phragmoplast generation irrespective of the position of the mitotic spindle or nuclei. These results indicated that MFs are indispensable for CMT reorganization at the M/G_1 interface, and supported my hypothesis of tubulin recruitment on the mode of CMT reorganization.

Chapter I

Visualization of microtubules by GFP-tubulin fusion protein in living plant cells

Introduction

In the initial stages of plant MT array research, transmission electron microscopy (Gunning and Hardham 1982) was used to provide "distinct" images in which the MTs could be clearly observed but only in a limited, two-dimensional view. A major breakthrough was achieved using immunocytochemistry and fluorescence microscopy or CLSM, through which exclusive images of MTs in whole cells could be observed (Lloyd 1987). Using these techniques, higher plant cells were found to posses four characteristic MT structures; the CMT array in interphase, PPB in late G_2 phase, the mitotic spindle in metaphase, and the phragmoplast in telophase (Lloyd 1987, Staiger and Lloyd 1991, Goddard et al. 1994). Although it had been speculated that MTs dynamically changed their structure during the cell cycle, the minute changes during the transitional phases could not be followed, since only fixed cells could be stained using anti-tubulin antibodies. Therefore, another experimental system was required to observe the reorganization of MTs in living cells, and various methods were tested.

The second major breakthrough was achieved by the use of the microinjection technique, by which fluorescent-labeled tubulin was microinjected into living plant cells. Carboxyfluorescein-labeled pig-brain tubulin, microinjected into the stamen hair cells of *Tradescantia*, progressively stained several MT structures, notably the PPB, mitotic spindle, and phragmoplast in single living cells throughout mitosis and cytokinesis (Zhang et al. 1990). However, only CMTs could not be observed in this study. Later, an extension of the microinjection method enabled the study of CMT arrays in living plant cells (Cleary et al. 1992, Wasteneys et al. 1993, Yuan et al. 1994, Wymer et al. 1997), thus not only allowing the observation of MT structures, but in combination with fluorescence redistribution after photobleaching (FRAP), permitted the analysis of MT turnover kinetics. The PPB,

phragmoplast, and interphase CMTs were consequently found to be highly dynamic, with turnover rates that were 3 to 4-fold faster than the interphase MTs of animal cells, whereas the spindle MTs exhibited similar kinetics to those of animal cells (Hush et al. 1994). Although the microinjection method made considerable distributions to our understanding of MTs in higher plant cells, it was still limited by the number of cells examined, and by the observation time which, due to technical difficulties, was restricted to a few hours.

The more recent use of fusion proteins between GFP and cytoskeletal proteins has enabled the visualization of these proteins and of cytoskeletal dynamics in living cells (Ludin and and Matus 1998). A MT reporter gene, constructed by fusing GFP to the microtubule-binding domain (MBD) of the mammalian microtubule-associated protein 4 (MAP4) gene, was introduced into the epidermal cells of *Vicia* by particle bombardment (Marc et al. 1998). The recombinant protein was transiently expressed, allowing rearrangements in the CMTs to be visualized for several days. However, the expression levels of the fusion protein were found to vary within each cell, with high levels of expression potentially inhibiting normal MT functions. A clear requirement therefore was stable transgenic plants expressing the reporter construct at appropriate levels - a possibility achieved by the introduction of gene constructs into plant cells by *Agrobacterium* mediated infection. Hence, a GFP-TUA6 (α-tubulin 6) fusion protein, stably expressed in transgenic *Arabidopsis* plants, was found to be incorporated into CMTs mainly in epidermal cells (Ueda et al. 1999, Ueda and Matsuyama 2000). Detailed time-lapse observations further revealed that short, randomly oriented MTs appeared at the first phase of CMT rearrangement from the transverse to longitudinal direction. Another report described the appearance of brightly fluorescent "knots" when CMTs branched or became reoriented to a deviating direction in trichomes of stably transformed *Arabidopsis* expressing a GFP-MBD fusion protein (Mathur and Chua 2000). These subtle and temporal MT structures were discovered by observations of living plants that stably expressed the GFP fusion proteins. Despite such reports of CMT reorientation, the rearrangements in MT structures could not be followed throughout mitosis, when the MT arrays were changing most dynamically, since very few cells

underwent cell division in the hypocotyls or trichomes. In order to investigate the events involved in MT rearrangement during mitosis, a high population of mitotic cells was required.

In this study, I have succeeded in establishing a transgenic BY-2 cell line that stably expresses a GFP-α-tubulin fusion protein, designated as BY-GT16, which could be highly synchronized by the drug treatment. Using the BY-GT16 cells, I also succeeded in monitoring MT dynamics throughout mitosis. The significance of these data is discussed.

Materials and Methods

Cell culture and synchronization of tobacco BY-2 cells

Cell culture and synchronization of tobacco BY-2 cell suspensions were performed as described by Nagata et al. (1992). Briefly, at weekly intervals, suspension cultures of a tobacco BY-2 cell line, derived from a seedling of *Nicotiana tabacum* L. cv. Bright Yellow 2, were diluted 95-fold with a modified Linsmaier and Skoog medium (Linsmaier and Skoog 1965). The cell suspension was agitated on a rotary shaker at 130 rpm at 27 °C in the dark. For synchronization of the cell cycle, 10 mL of 7-day-old cell suspensions were transferred to 95mL of the fresh medium and cultured for 24 h with 5 mg/L aphidicolin (Sigma Chemical Co., St. Louis, MO, U.S.A.). The cells were thoroughly washed with 10 volumes of the fresh medium and resuspended in fresh medium. The cells were harvested hourly from 0 to 13 h after the release from aphidicolin to allow examination of each stage between the S and G_1 phase.

GFP-tubulin construct, transformation and selection of transformants

A tobacco α-tubulin cDNA was isolated from 2-day-old BY-2 cDNA library (Ishida et al. 1993) using *Arabidopsis* α-tubulin cDNA (*TUA3*; kindly supplied by Dr. Snustad of University of Minnesota) as a probe. The tobacco cDNA was inserted between the *BsrG*I and *Not*I sites of the CaMV 35S-sGFP (S65T) vector (kindly supplied by Dr. Niwa of University of Shizuoka), resulting in an in-frame fusion between sGFP and the TUA, connected by an

Ala-Gly linker. The GFP-tubulin fusion sequence was then inserted between the *BamH*I and *Not*I sites of the modified pBI121 binary vector (Clontech Laboratories, Inc., Palo Alto, CA, U.S.A.), in which the *Not*I site was inserted between the *BamH*I and *Sac*I sites in advance, thus placing the inserted sequence upstream of the Nos terminator. *Agrobacterium tumefaciens strain*, LBA4404, was transformed with this construct, and a 4 mL aliquot of 3-day-old BY-2 cells were inoculated with 100μL of an overnight culture of this transformant as described by An (1995). After 2-day incubation at 25 °C, the cells were washed four times in 5 mL of LS medium, and were then plated onto solid LS medium containing 500mg/L carbenicillin and 200mg/L kanamycin. Calluses, which appeared after 10 days, were transferred onto new plates and were cultured independently.

Establishment and observations of the BY-2 cell line expressing the GFP-tubulin protein

Independent calluses of about 1 cm in diameter were transferred to 20 mL liquid LS medium in 100 mL Erlenmeyer flasks and agitated on a rotary shaker at 130 rpm at 27 °C in the dark. After one month, the cell lines suitable for MT observations were selected by identifying GFP-fluorescent cells by fluorescence microscopy. The cell lines, designated as BY-GT (BY-2 cells stably expressing a GFP-Tubulin protein), were selected and their growth rates accelerated by several methods as described in the Results. Finally, a cell line (BY-GT16) with the most desirable features for purpose was obtained. The BY-GT16 cells could be maintained 95-fold dilution at weekly intervals in LS medium with KH_2PO_4 concentration increased to 470 mg/L. The GFP fluorescence localized at MT was clearly observable in living BY-GT16 cells. For time-sequential observations, 2-day-old BY-GT16 cells were transferred into ϕ35 mm Petri dishes with ϕ14 mm cover slip windows at the bottom (Matsunami Glass Lnd., Ltd., Osaka, Japan). The dishes were placed onto the inverted platform of a fluorescence microscope (IX, Olympus Co. Ltd., Tokyo, Japan) equipped with a confocal laser scanning head and control systems (GB-200, Olympus). This observation system, which allows us to observe the MT dynamics of BY-GT16 cells with minimal damage, was found to be ideal for these studies. The images of the cells were

processed digitally, using Photoshop software (Adobe Systems Inc., San Jose, CA, U.S.A.).

Immunocytochemistry

For staining of MTs, the cells were treated with 250 μM *m*-maleimidobenzoyl-*N*-hydroxysuccinimide ester (MBS; Pierce Chemical Co., Rockford, IL, USA) dissolved in 50 mM PIPES buffer (pH 6.8) containing 1 mM $MgSO_4$, 5 mM EGTA and 1 % glycerol (PMEG) for 30 min prior to fixation (Hasezawa and Nagata 1991). The cells were fixed with 3.7 % (w/v) formaldehyde dissolved in PMEG buffer for 1 h and then placed onto cover slips coated with poly-L-lysine. The cells were treated with an enzyme solution containing 1% cellulase Y-C and 0.1% pectolyase Y-23 for 5 min, followed by washing with PMEG buffer. Subsequently, treatment with a detergent solution containing 1 % IGEPAL CA-630 was performed for 15 min, followed by washing with phosphate-buffered saline (PBS; 20 mM Na-phosphate and 150 mM NaCl, pH 7.0). The cells were then treated with a glycine solution (0.1 M glycine, 1 % Bovine Serum Albumin and 0.005 % Triton X-100 in PBS) for 10 min, followed by washing with PBS. The cells were then stained with a solution of 20 μg/l 4',6-diamidino- 2-phenylindole (DAPI) for 5 min. To stain MTs, the cells were treated with a mouse anti-α-tubulin antibody (Oncogene Research Products, Boston, USA), and then with a rhodamine-conjugated goat anti-mouse IgG secondary antibody (Sigma) both for 30 min. Finally, the cells were washed five times with PBS and embedded in a glycerol solution containing an anti-fading reagent (SlowFade Light, Molecular Probes, Eugene, OR, USA). Specimens were examined under the CLSM as described above.

Transmission electron microscopy

For transmission electron microscopy, BY-GT16 cells were pre-fixed with 4 % glutaraldehyde for 1 h at room temperature by addition of 2 mL of 8 % glutaraldehyde in 3mM HEPES buffer (pH 7.0) to 2 mL of cell suspension. The cells were then rinsed with 6 mM HEPES buffer (pH 7.0) for 2 h, and post-fixed in 2 % OsO_4 in 6 mM HEPES (pH 7.0) for 2 h at room temperature. The fixed materials were then dehydrated through an ethanol

series and propylene oxide, and subsequently embedded in Spurr's resin (Spurr 1969). Sections were cut with a Diatone diamond knife on an Ultracut UCT (Leica, Wien, Austria) and stained with uranil acetate and lead citrate. Preparations were viewed with a JEM-1010 electron microscopy (JEOL, Tokyo, Japan).

Results

Transformation of BY-2 cells by the GFP-tubulin construct

To first obtain the gene encoding α-tubulin from tobacco, a cDNA library of tobacco BY-2 cells was screened using the *Arabidopsis TUA3* gene as a probe. The identified cDNA, which was called *NtNUA*, consisted 1,659 bp and encoded a putative protein of 450 residues with a calculated molecular mass of 49,707 (DDBJ accession number, AB052822). This protein showed 95 % identity to the *Arabidopsis* AtTUA6 protein. Subsequently, tobacco BY-2 cells were transformed by *Agrobacterium* harboring the 35S-GFP-tubulin construct in pBI121 (Fig. I-1), essentially as described by An (1995). From this transformation, I obtained 16 independent clones, which were maintained separately on solid modified-LS medium. In the current experiments, I used only clone 16, as it showed sufficient fluorescence at the solid culture stage, when examined by fluorescence microscopy. After several subcultures through agar medium, the clone was transferred to liquid modified-LS medium as described above.

Establishment and characterization or the transformed cell line

Since shortly after transfer to liquid medium the cell line formed small clumps, they were repeated filtrated through 1 mm pore-sized stainless-steel meshes in order to produce fine cell cultures suitable for observing GFP-labeled MTs of the cells. Subsequently, to enhance their growth rates, 15 mL of the stationary stage cells were transferred to 80 mL fresh medium, with the results that the cells could reach the stationary phase stage in 4 days. After 3 to 4 repeats of this treatment, the resulting transformed cell line, designated as BY-GT16 (BY-2 cells stably expressing a GFP-Tubulin protein clone 16) and showing the

bright GFP-fluorescence compared to the original BY-2 cells, could be maintained by 95-fold dilutions at weekly intervals as described above. The growth rate of the cell line increased to that comparable to the original tobacco BY-2 cells (Fig. I-2A). The BY-GT16 cells could also be synchronized by the same method using aphidicolin as for the original BY-2 cells. Actually, the BY-GT16 cells showed single peaks as high as 60 % mitotic index (MI) at 9.5h after release from aphidicolin (Fig. I-2B) and about 80 % MI by sequential treatment with aphidicolin and propyzamide (data not shown). Noticeably, the peak time of MI is same as that of the original BY-2 cells, indicating that cell cycle progression and growth speed of BY-GT16 cells were quite comparable to those of the original BY-2 cells.

The shapes and size of the BY-2 cells and BY-GT16 cells were indistinguishable (Fig. I-3A, B). However, the BY-GT16 cells emitted bright GFP-fluorescence, which highlighted the gross morphology of the mitotic apparatus (Fig. I-3C). The observed features were similar to those observed by staining BY-2 cells with anti-tubulin antibodies. Therefore, the fused TUA protein used here appeared to be incorporated evenly into the MT structures. The immunoblot analysis revealed that the amount of the fusion protein was less than one-tenth of that of the endogenous α-tubulin, and there was no obvious effect on the endogenous tubulin expression level (data not shown). The BY-GT16 cells also showed similar growth rates, and 10-20 % of 2-day-old cells were observed in the M phase (Fig. I-3D). The cells could also synchronized, and therefore, at the peak of MI, a large number of cells at various mitotic and premitotic stages could be easily observed at one time (Fig. I-3E, F).

Cell cycle progression and microtubule dynamics of BY-GT16 cells

The MTs were stained and observed by immunocytochemical techniques using anti-tubulin andibodies and rhodamine-labeled secondary antibody to ensure that the GFP-fluorescence of BY-GT16 cells really represented the MTs. The structures shown by GFP-fluorescence and rhodamine-fluorescence were almost overlapping in the CMTs (Fig. I-4A, B), the PPB (Fig. I-4C, D), the spindle (Fig. I-4E, F) and the phragmoplast (Fig. I-4G, H). The MTs observed by transmission electron microscopy also showed no abnormalities (Fig. I-4I, J). These results

suggested that the dynamic changes in MT configurations of BY-GT16 cells progressed normally, and could thus be followed by real-time observations of GFP-fluorescence.

During the M phase, when various events of cell division occur within a short time period, it is especially important to observe MT dynamics, since MT structures play important roles in such events. The cell synchronization systems using BY-GT16 are considered very useful for studying various events during cell cycle progression. Indeed, using BY-GT16 cells, the dynamic changes of MTs configurations could be followed in a certain number of cells at the same optical frame under the CLSM. In this observation system, all the cells progressed normally from the late G_2 phase to the early G_1 phase (Fig. I-5) without any disturbance, as determined by scans performed for 160s at 10 min intervals using an x20 dry objective (UPlanFl, Olympus). In this case, the total observation time was over 3 h, and the period of M phase was estimated to be about 2 h. As this period closely corresponded to that of the original BY-2 cells (Nagata et al. 1992), it could be concluded that the observed cell had not been injured by the fluorescence used for the observations, and that cell cycle progression had not been retarded significantly compared to original cell line. Therefore, using this system, the mitotic events involving MTs could be studied in detail. For example, it was observed, as shown arrowheads in Fig. I-5, that the double PPBs actually induced the oblique cell plate as previously reported (Hasezawa et al. 1994, Yoneda et al. 2005). Within a single cell, the formation and disappearance of the PPB, spindle and phragmoplast were clearly recognizable in this order (Fig. I-6). Subsequently, the short MTs began to be formed in the perinuclear regions.

Discussions

The MTs are known to play important roles during cell cycle progression in higher plant cells. Therefore it is important to understand the mechanisms of MT structural changes. To follow these processes, it is preferable to observe such dynamics in a non-invasive manner. I have shown in this study that tobacco BY-2 cells, stably transformed by a *GFP-NtTUA* gene construct by agroinfection, could grow as rapidly as the original

non-transformed BY-2 cells. Most notably, the transgenic BY-GT16 cell line could be highly synchronized by aphidicolin, reaching an MI of 60 %, thus allowing the process of cell cycle transition to be studied in detail.

The unique observation system with BY-GT16 cells can be applicable to various investigations of cell cycle events involving MTs. For example, changes of MT structures could be minutely observed in the synchronized BY-GT16 cells, and the average times both in metaphase and anaphase could be estimated as about 20-30 min. In addition, using BY-GT16 cells, our laboratory reported that PPB predicted the future division site, because the division plane certainly connected where the PPB had existed (Hoshino et al. 2003). The PPB site and later division plane were directly observed in the same BY-GT16 cells. While PPB shows a single ringed structure in usual, double PPBs were sometimes observed in elongated BY-2 cells, and resulted in oblique phragmoplast and division plane (Hasezawa et al. 1994). BY-GT16 cells also became applicable to detail investigation of PPB in forming spindle poles and determining division plane (Yoneda et al. 2005). Furthermore, it could be performed to follow the organization of cytoplasmic MTs from the perinuclear region at the G_1/S interface, and to compare these results with previous observations in our lab (Miyake et al. 1997). In any case, using the BY-GT16 cells, the whole MT dynamics can be followed throughout the cell cycle.

Similarly, recent reports on the fate of MT reorganization using GFP confirmed the observations in this study that MTs are organized on the nuclear surface at the M/G_1 interface (Hasezawa et al. 2000, Granger and Cyr 2000). Furthermore, Hasezawa et al. (2000) reported that, using *Arabidopsis* cell suspensions expressing *GFP-TUA6*, MTs from nuclei elongated and reached the cell cortex, although the later process could not be sufficiently followed, probably because the *Arabidopsis* suspension cultured cells were too small in cell size to observe CMT reorganization and could not be highly synchronized. Although Granger and Cyr (2000) used BY-2 cell line expressing *GFP-MBD*, which seemed to be large enough to observe CMTs, the peak of MI in cell synchronization was low as 20 %, and the GFP-fluorescence was very weak so that MTs could not be observed in naked eyes,

most probably because of the low expression level of GFP-MBD fusion protein, and the use of a heterogeneous, mammalian MAP4 protein. In contrast, BY-GT16 cells, expressing *GFP-NtTUA*, showed very bright GFP-fluorescence and could be synchronized as high as 60 % at the peak of MI. Therefore, the BY-GT16 cell line that was established in this study could be useful to follow CMT reorganizing processes. Indeed, using the BY-GT16 cells, I succeeded in detail observations of CMT reorganization at the M/G_1 interface, and will report them in the next chapter.

Figures

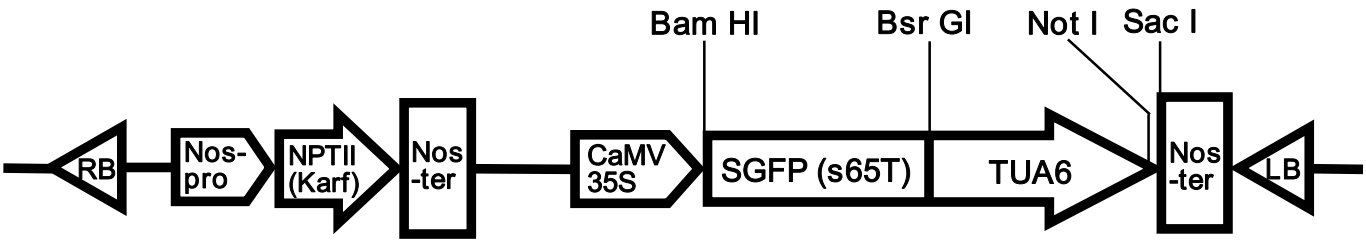

Fig. I-1 The *sGFP-TUA* construct used for BY-2 transformation. The construct consists of the *sGFP-TUA* sequence placed between *35S* (CaMV *35S* promotor) and *Nos ter* (nopaline synthase terminal polyadenylation signal) and the *NPTII* gene (neomycin transferase providing kanamycin resistance) placed between *Nos pro* (nopaline synthase promotor) and *Nos ter*.

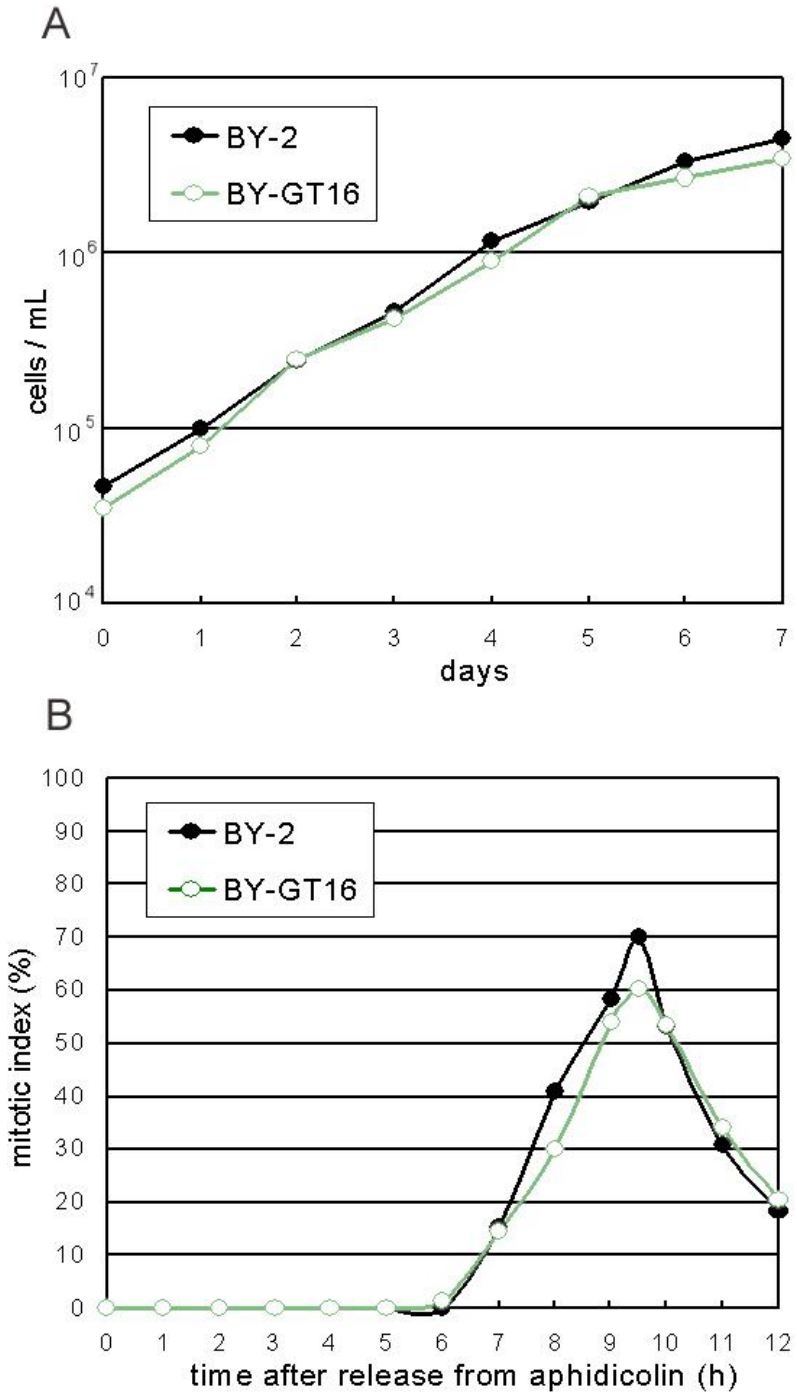

Fig. I-2 Characterization of original BY-2 and transformed BY-GT16 cells. Both cell line grew about 100-fold in a week (A). When cells were synchronized by aphidicolin treatment, mitotic index of BY-GT16 cells (green open circle) reached 60 % at 9.5 h after release from aphidicolin, and the peak time is same as that of BY-2 cells (black closed circle).

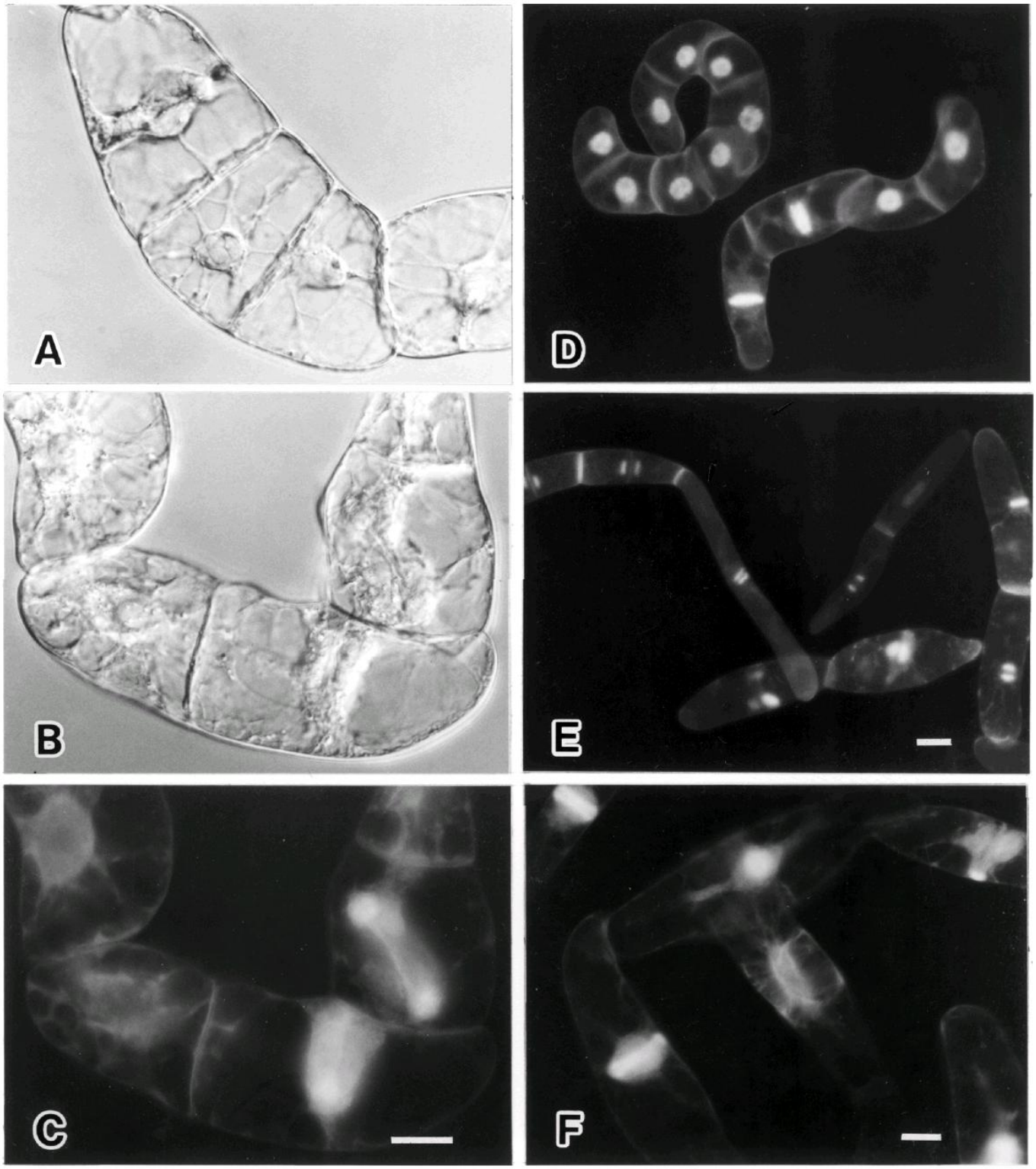

Fig. I-3 Cell suspensions of original BY-2 and transformed BY-GT16 cells. Two-day-old BY-2 (A) and BY-GT16 cells (B). The same cells as in (B) showed the bright fluorescence of GFP-tubulin of the phragmoplast and cytoplasmic MTs under fluorescence microscopy (C). Two-day old (D) and synchronized BY-GT16 cells at ca 60 % MI peak (E) stained with DAPI. GFP-fluorescence of the mitotic apparatus of the synchronized BY-GT16 cells at the peak MI (F). Bars represent 10μm.

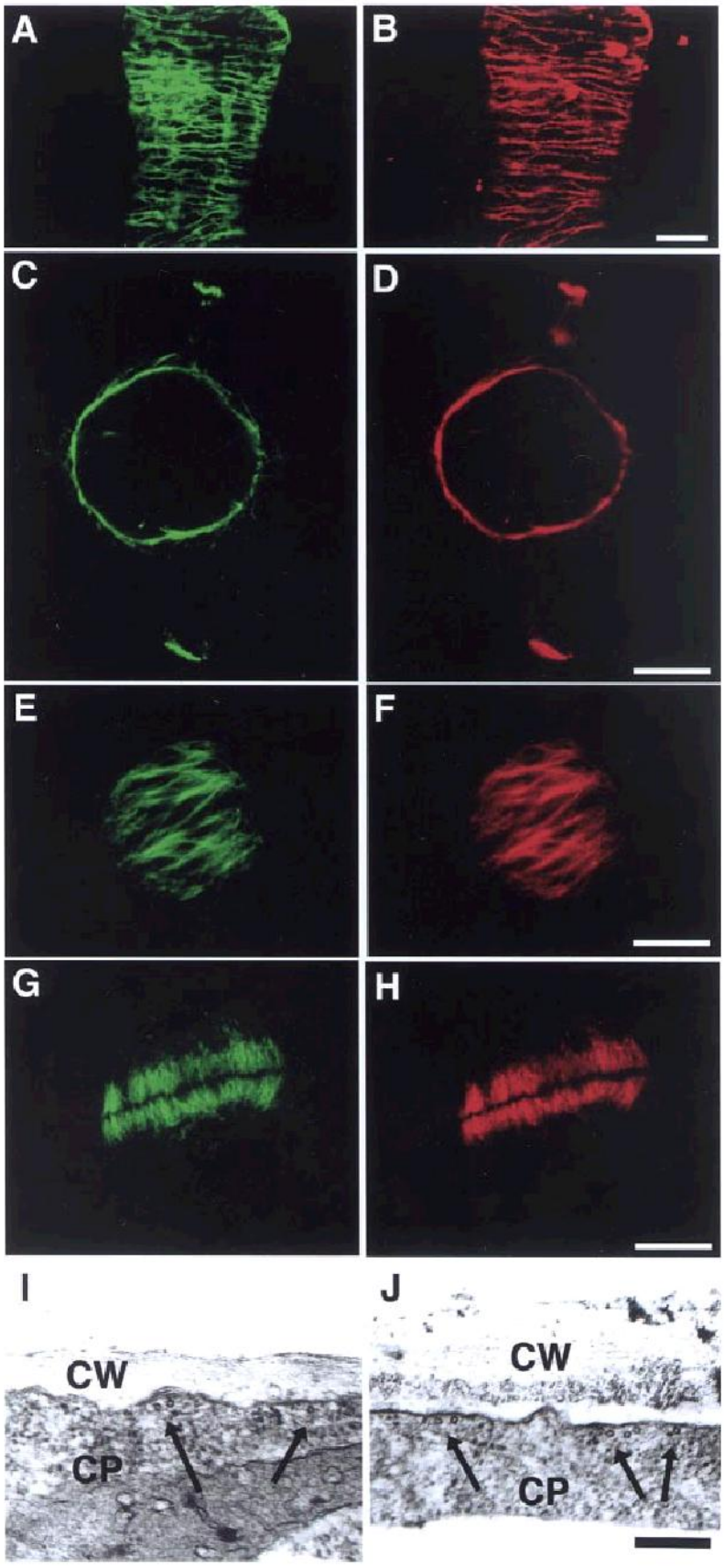

Fig. I-4 Microtubules in BY-GT16 cells. BY-GT16 cells, stained with anti-tubulin antibodies and rhodamine-conjugated secondary antibody, showing structures with GFP-fluorescence (A, C, E, G) and rhodamine-fluorescence (B, D, F, H). The CMTs (A, B), PPB (C, D), spindle (E, F) and phragmoplast (G, H) were similarly stained. CMTs of the BY-2 cell (I, arrows) and those of BY-GT16 (J, arrows), observed by transmission electron microscopy, were indistinguishable. CW, cell wall; CP, cytoplasm. Bars represent 10 μm (A-H) and 200 nm (I, J)

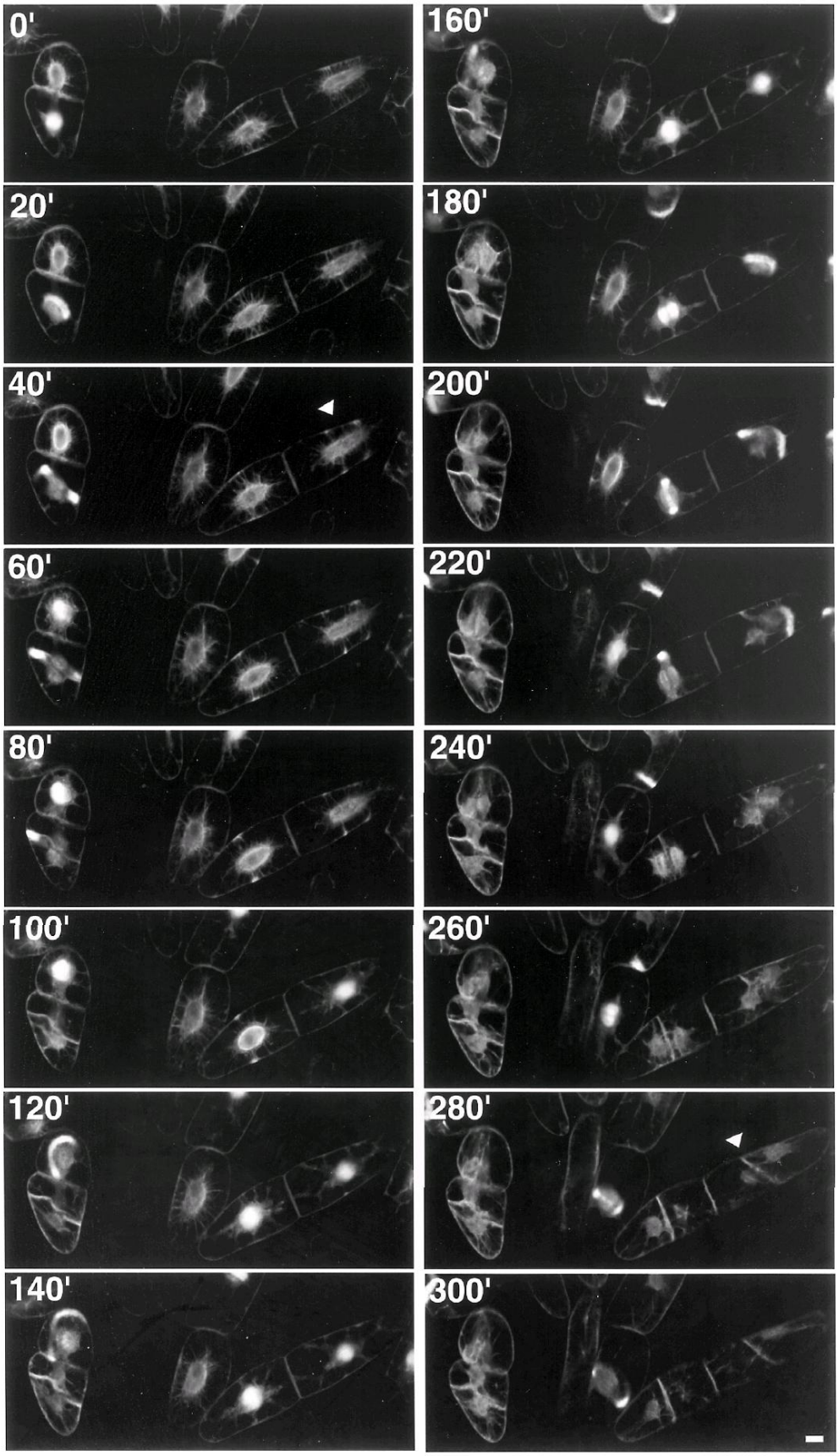

Fig. I-5 Time-sequence observations of the dynamic changes in the mitotic apparatus of BY-GT16 cells by a time-lapse CLSM system throughout mitosis. The scans were performed at 10 min intervals, for a total of over 3 h. The series of figures shown here are at 20 min intervals. In each cell, development and disappearance of the PPB, change of the spindle, development and collapse of the phragmoplast, and reorganization of CMTs were observed in this order. The double PPBs (arrowhead in 40 min) actually induced the oblique cell plate (arrowhead in 280 min). Bar represents 10 μm.

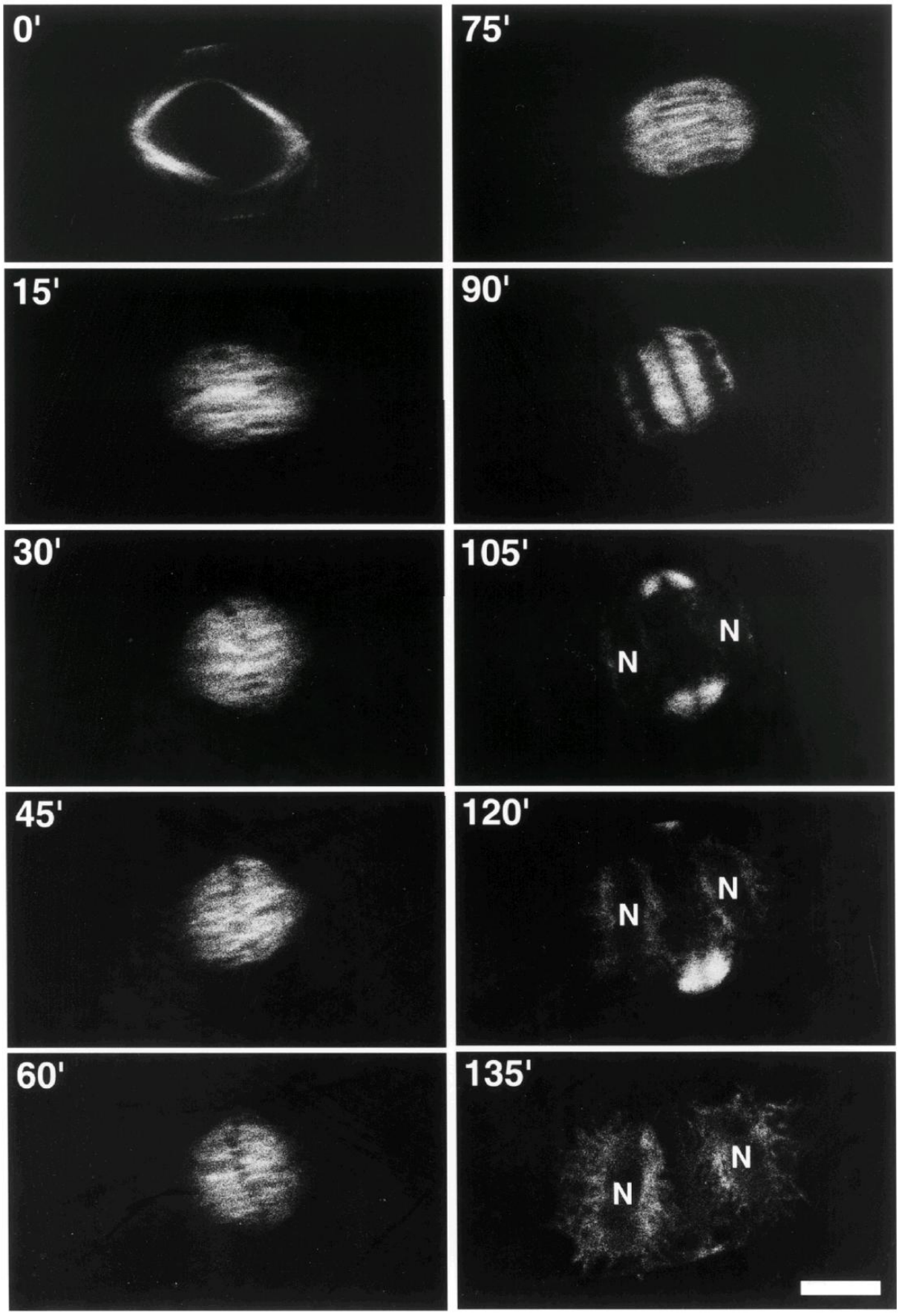

Fig. I-6 Time-sequence observations of the dynamic MT changes of a single BY-GT16 cell by a time-lapse CLSM system throughout mitosis. The scans were performed at 15 min intervals in a single optical section. 0-30 min, the spindle was developing from prophase to metaphase; 45-75 min, the spindle was changing from metaphase to anaphase; 90-105 min, the phragmoplast was growing; 120-135 min, the short MTs were performed in the perinuclear region. Bar represents 10 μm. N, Nuculeus.

Chapter II

Analysis of cortical microtubule reorganization at the M/G_1 interface in living plant cells

Introduction

In higher plant cells, the characteristic structures of MTs; the CMTs, the PPB, the mitotic spindle, and the phragmoplast MTs, appear in turn during cell cycle progression. Of these structures, the CMTs have been implicated in the morphogenesis of plant cells by regulating the orientation of newly deposited CMFs. Accumulating evidence suggests that the ordered CMTs affect the patterns of CMF deposition on the plant cell surface by controlling the movement of cellulose-synthesizing complexes within the fluid mosaic membrane, and that the deposition patterns of newly-synthesized CMFs determine the cell shape (Baskin 2001). The structural changes in the configurations of CMTs are therefore considered to be dynamic and to be closely associated with plant morphogenesis.

The CMTs are decomposed at the G_2/M interface and then become reorganized at the M/G_1 interface. To gain insights into this reorganization of CMTs, the use of tobacco BY-2 cells has proved invaluable, particularly as they can be highly synchronized by drug treatment (Hasezawa and Nagata 1991, Nagata et al. 1992). In earlier studies, the changes in MT structures of BY-2 cells were extensively examined by immunocytochemical techniques after fixation (Hasezawa and Nagata 1991, Nagata et al. 1994, Hasezawa et al. 1997). In particular, the events during cell cycle progression from M phase to the G_1 phase was determined with this system, which thus allowed the mode of CMT organization, first on the nuclear surface and then on the cell cortex, to be determined (Hasezawa and Nagata 1991, Nagata et al. 1994). However, the previous hypotheses of the reorganization events were based on statistical data obtained from observations of fixed cells. More direct evidence, for example from time-sequential observations of living cells, was required to confirm the process.

Visualization of MTs in living plant cells for several hours after microinjection of

florescent-labeled tubulin provided some new data on MT dynamics and kinetics (Zhang et al. 1990, Wasteneys et al. 1993, Hush et al. 1994). However, technical difficulties with the method limited the number of treated cells and the observation time. More recently, the labeling of proteins with GFP has become a common method in cell biology. This method has also been applied to cytoskeletal proteins, allowing the dynamic behavior of MTs to be examined in detail in living plant cells. A fusion protein with GFP and the MBD of MAP4, which was transiently expressed in epidermal cells of *Vicia faba* bean following particle bombardment, allowed the rearrangement of CMTs to be observed for a few days (Marc et al. 1998). However, the brightness and intensity of the GFP fluorescence varied between cells, and some MT structures appeared to have been affected by MBD overexpression. The use of *Agrobacterium*-mediated, stable transformed plants may provide a more suitable system for investigating MT dynamics. In this context, the rearrangement of CMTs in *Arabidopsis* plants expressing a GFP-tubulin (Ueda et al. 1999, Ueda and Matsuyama 2000) and the reorientation of MTs in *Arabidopsis* cells stably expressing GFP-MBD (Mathur and Chua 2000) have been reported. In an earlier study, for the first time in living higher eukaryotic cells, MT dynamics throughout mitosis, from the late G_2 phase to the early G_1 phase, was demonstrated (Hasezawa et al. 2000). In this observation system, however, CMT reorganization at the M/G_1 interface could not be followed in greater detail because the *Arabidopsis* cells were small in size and could not be highly synchronized. More recently, I have newly established BY-2 cell line that stably expresses the GFP-tubulin fusion protein (BY-GT16) (Chapter I and Kumagai et al. 2001). In this study, using the BY-GT16 cells, I attempted to clarify the processes of CMT reorganization at the M/G_1 interface.

Despite the numerous reports of MT dynamics as structural changes of fibrous MTs, there have been very few direct observations of the movement of tubulins as a constituent of MTs. In this study, therefore, I attempted to observe the movement of GFP-tubulin and MT nucleation. Indeed, I was able to identify the accumulation and movement of GFP-tubulin on the nuclear surface after phragmoplast collapse, and subsequently the translocation of tubulin up to the development of nascent MTs from the nuclear surface. I have also been

able to provide direct evidence for the earlier hypothesis that, during cell cycle transition from M phase to the G_1 phase, five sequential sub-phases (I II, III_a, III_b and III_c) can be observed by immunofluorescence microscopy after staining with anti-tubulin antibodies (Nagata et al. 1994). Furthermore, I observed that after MT organization on the nuclear surface and their elongation to the cell cortex, the MTs became transiently parallel to the long axis of the cells, and then the transverse MTs formed at the site close to the division plane. In addition, observations of these BY-GT16 cells demonstrated that when the MTs nucleated from the daughter nuclei reached the cell cortex (from I to II), they appeared as bright spots on the cortex from which the parallel CMTs would become organized. These steps in tubulin migration and CMT reorganization, involving what had not been identified prior to this study, are discussed in relation to the previous understanding of the reorganization of CMTs during cell cycle transition from the M phase to G_1 phase.

Materials and Methods

Plant material and Synchronization

Suspension cultures of a BY-GT16 (BY-2 cells expressing GFP-tubulin fusion protein clone 16) cell line were maintained similar to the tobacco BY-2 cell line. Briefly, at weekly intervals, suspension cultures of the BY-GT16 cell line were diluted 95-fold with a modified Linsmaier and Skoog medium, as described by Nagata et al. (1992). The cell suspension was agitated on a rotary shaker at 130 rpm at 27 °C in the dark. For synchronization of the cell cycle, 10 mL of 7-day-old BY-GT16 cells were transferred to 95 mL of fresh medium and cultured for 24 h with 5 mg/L aphidicolin (Sigma Chemical Co., St. Louis, MO, U.S.A.). The cells were washed with 10 volumes of the medium and then resuspended in fresh medium (Hasezawa and Nagata 1991, Nagata and Kumagai 1999). The peak mitotic index (MI) of ca. 60 % could be observed at 9.5~10 h after release from aphidicolin (Chapter I and Kumagai et al. 2001).

Time-sequence observations and spatial analysis of BY-GT16 cells using deconvolution

microscopy or CLSM.

Co-localization of GFP fluorescence and tubulin molecules was clearly observed in living BY-GT16 cells. For time-sequence observations, the synchronized or 3~4-day-old BY-GT16 cells were transferred into ϕ35 mm Petri dishes with poly-L-lysine-coated ϕ14 mm coverslip windows at the bottom (Matsunami Glass Ind., Ltd., Osaka, Japan). The dishes were placed onto the inverted platform of a fluorescence microscope (IX, Olympus Co. Ltd., Tokyo, Japan) equipped with a confocal laser scanning head system (GB-200, Olympus) or a cooled CCD camera head system (CoolSNAP HQ, PhotoMetrics Inc., Huntington Beach, Canada). Using the latter system, the Z-stack figures acquired were deconvoluted by AutoDeblur software (AutoQuant Imaging Inc., California, USA) to digitally show the optical sections, which were then 3D-reconstructed using MetaMorph software (Universal Imaging Co., Downingtown, Panama). Subsequently, the images were digitally processed, using Photoshop software (Adobe Systems Inc., California, USA).

Immunocytochemistry

For staining of MTs, the BY-GT16 cells were treated with 250 μM m-maleimidobenzoyl-N-hydroxysuccinimide ester (MBS; Pierce Chemical Co., Rockford, IL, U.S.A.) for 30 min prior to fixation. They were fixed with 3.7 % (w/v) formaldehyde for 1 h and then placed onto coverslips coated with poly-L-lysine. The cells were then treated with an enzyme solution containing 0.1 % pectolyase Y23 and 1 % cellulase Y-C (both from Seishin Co., Tokyo, Japan) for 5 min, followed by washing with PMEG solution (50 mM PIPES, 1 mM $MgSO_4$, 5 mM EGTA, and 1 % Glycerol, pH 6.8). Treatment with a detergent solution containing 1 % Nonidet P-40 was then performed for 15 min as described in Hasezawa and Nagata (1991), followed by washing with phosphate-buffered saline (PBS; 20 mM Na-phosphate and 150 mM NaCl, pH 7.0). The cells were then incubated with antibodies against tubulins (1:1 mixture of mouse anti-α-tubulin and anti-β-tubulin; Amersham Co., Buckinghamshire, UK) to stain MTs or clone G9 antibody (mouse monoclonal antibody raised against *Schizosaccharomyces pombe* γ-tubulin; Kumagai et al.

2003) to stain γ-tubulin for 1 h, washed with PBS, and then incubated with a rhodamine-conjugated goat anti-mouse antibody (Cappel Co., West Chester, PA, U.S.A.) for 1 h, followed by washing with PBS. After DNA staining with 4,6-diamidino- -phenylindole (DAPI), the cells were finally embedded in a glycerol solution as described by Hasezawa and Nagata (1991). All procedures described above were performed at room temperature. The cells were subsequently observed by CLSM or deconvolution microscopy as described above.

Results

Observations of MT structures in BY-GT16 cells during the cell cycle.

I have established BY-GT16 cell line (BY-2 cell line stably expressing GFP-Tubulin clone 16) by *Agrobacterium*-mediated transformation of tobacco BY-2 cells with the 35S-GFP-tubulin construct as described in Chapter I and Kumagai et al. (2001). BY-GT16 cells, showing bright GFP-fluorescence of their MT structures, could be maintained by 95-fold dilutions at weekly intervals and could be synchronized by the same method as for the original BY-2 cells using aphidicolin. Furthermore, the shapes and sizes of the BY-GT16 cells were also indistinguishable from those of the BY-2 cells. As the observed BY-GT16 features were similar to those observed by staining BY-2 cells with anti-tubulin antibodies, the fused TUA protein used here appeared to have been evenly incorporated into the MT structures. Immunoblot analysis revealed that the amount of fusion protein was less than 10 % that of the endogenous α-tubulin, with no obvious effects on endogenous tubulin expression levels (data not shown). As all of the MT structures, including the PPB, mitotic spindle, phragmoplast, CMTs and cytoplasmic MTs could be observed (Fig. II-1), I considered the BY-GT16 cell-synchronization system to be extremely useful for studying various MT events during cell cycle progression.

Spatial analysis of tubulin movement and MT nucleation in BY-GT16 cells

I found that a deconvolution microscope system was suitable for spatial analysis and obtaining clear 3D images of whole cell events. In this study, therefore, each BY-GT16 cell

was observed from the cell cortex to the mid-plane and was analyzed spatially by deconvolution microscopy; thus allowing me to observe the MT dynamics of BY-GT16 cells with minimal damage. In particular, I was able to perform minute spatial and time-sequential observations because the cooled CCD camera of the deconvolution microscopy system required short exposure times. In this system, each cell could be photographed from the cortex to mid-plane with 2 or 3 min interval. The photo-data was then processed using blind deconvolution to obtain serial optical sections and subsequently reconstructed to form 3D images. By examining the conditions of the photographs and the deconvolution calculations, the translocation of tubulin could be time-sequentially followed, from phragmoplast collapse to CMT reorganization at the M/G_1 interface, by observing GFP fluorescence (Fig. II-2). As a result, the final remnant of the phragmoplast gradually became to be observed not as fibrous MTs but rather as an ambiguous area of GFP fluorescence (Fig. II-2a, 0-8 min). From there, the GFP fluorescence accumulated at the nuclear surface near the cell plate (Fig. II-2a, 8-10 min, arrows), and subsequently also on the opposite side of the nuclear surface (Fig. II-2a, 12 min, arrow), where the nascent MTs elongated (Fig. II-2a, 16-18 min, arrowheads). Most of tubulin seemed accumulate at the nuclear surface near the cell plate (Fig. II-2a, 8-10 min, arrows), however, a slight sign of accumulation could also be seen at the opposite side at 8-10 min. In another example of a BY-GT16 cell, observed from a side angle to the remnant of phragmoplast (Fig. II-2b), the GFP fluorescence appeared to accumulate from the phragmoplast remnant onto the nuclear surface near the cell plate (Fig. II-2b, 0-2 min, arrows). When the accumulation of fluorescence appeared on the opposite side of nucleus, a bridge of GFP-tubulin fluorescence (Fig. II-2b, 2-4 min, arrowheads) was observed between the two accumulation sites on the both sides of nucleus (Fig. II-2b, 2-4 min, arrows), but was no longer observed at 6 min. Subsequently, the nascent MTs nucleated from the site opposite the cell plate (Fig. II-2b, 8 min, arrowhead). From repeated observations, the nascent MTs were found to be necessarily organized within a short time-span after the appearance of fluorescence accumulation on the nuclear surface opposite the cell plate. Although more than 50 cell pairs were analyzed, no exception was observed in

the following order; phragmoplast collapsing, tubulin accumulation at the nuclear surface facing the cell plate, the accumulation at the opposite side of the nuclear surface, and the MT nucleation from there.

To gain further insights into tubulin translocation, I examined GFP fluorescence by comparison of the 3D images and figures from the optical plane (Fig. II-3). On the nuclear surface near the cell plate, connections of GFP fluorescence were observed from the remnants of the phragmoplast to the nuclear envelope (Fig. II-3, 4 min left, arrowheads). At the same time, the GFP fluorescence began to accumulate onto the mid-plane (Fig. II-3, 4 min middle, arrow). Moreover, the accumulation of GFP fluorescence was clearly observed in the 3D images constructed using figures from the cortex to the mid-plane (Fig. II-3, 4 min right, arrow). Thus, when the sites of accumulation of GFP fluorescence were observed on both sides of the nucleus (Fig. II-3, 8 min right, arrows), the bridges of fluorescence on the nuclear surface connected the two sites (Fig. II-3, 8 min left, arrowheads). At the same time, on the mid-plane, the MTs nucleated from the accumulation site opposite the cell plate and elongated to the cell cortex (Fig. II-3, 8-12 min middle, arrowheads). Each site of accumulation of GFP fluorescence seemed to consist of free tubulin, since it was not recognized as fibrous material but rather as an area, and was observed through several optical planes. With phragmoplast collapse, the tubulin became liberated and seemed to first accumulate at the nuclear surface near the cell plate, and then to accumulate again on the opposite surface of the nucleus, where it appeared to be recycled in order to organize the MTs.

To confirm the results obtained by GFP fluorescence, the BY-GT16 cells were stained with the anti-tubulin antibody and DAPI (Fig. II-4), and the following figures of tubulin distribution at the M/G_1 interface were obtained: a) remnant of phragmoplast, b) accumulation of tubulin on the nuclear surface near the cell plate, c) accumulation of tubulin on both sides of the nuclear surface, d) accumulation of tubulin on the nuclear surface opposite to the cell plate. When the immunofluorescent figures were compared with the figures of GFP fluorescence within the same cells, no clear differences could be observed

between them.

The accumulation sites of tubulin, especially at the opposite side of nuclear surface facing away from the cell plate, may act as MTOC (microtubule organizing center) sites. Therefore, the localization of γ-tubulin, which is known as a major component of MTOC, was investigated. The BY-GT16 cells were stained with the anti- γ-tubulin antibody (Fig. II-5). At the phragmoplast, anti- γ-tubulin antibody stained the outer sides of phragmoplast (Fig. II-5, a-c) as previously described (Kumagai et al. 2003). Around when the phragmoplast was collapsing, both α-tubulin and γ-tubulin gradually accumulated on the nuclear surface at the near side to the cell plate (Fig. II-5, d-f, arrow). However, when α-tubulin clearly accumulated there, γ-tubulin had already accumulated not only at the near side (Fig. II-5, g, small arrows) but also at the opposite side to the cell plate (Fig. II-5, h, large arrows). The α-tubulin accumulated to the accumulation sites of γ-tubulin (Fig. II-5, j-l, large arrows), where nascent MTs would elongate to the cell cortex.

Fate of the nascent MTs originated at the perinuclear region

To follow the MTs nucleated from the nuclei, BY-GT16 cells were observed by CLSM (Fig. II-6). When the focal plane was parallel to the elongating MTs, the thick bundles of MTs were elongated from the nuclear surface of the daughter nuclei and reached to the cell cortex (Fig. II-6a, arrows). When the transected optical sections were obtained, their thick bundles of MTs were connected to the cell cortex, and were observed as the bright spots on the cell cortex section (Fig. II-6b, arrows).

Time-sequential observations of CMT reorganization on the cell cortex in BY-GT16 cells

To observe the CMT reorganization in detail, time-sequential observations on the cell cortex of the BY-GT16 cells were performed by the CLSM. When remnants of the phragmoplast could still be observed, the nascent MTs were recognized on the nuclear surface of the two daughter cells (Fig. II-7, 0 min, midplane). In 0 min, no fibrous structures could be recognized except for the dim fluorescence that was assumed to originate from free

GFP-tubulin in the cytoplasm. After 9 to 18 min, the bright spots appeared on the cell cortex (Fig. II-7, 9-18 min, arrows) and from there the first CMTs elongated. The MTs were at first randomly oriented (Fig. II-7, 12-15 min, circle), but then parallel with, or at a slightly-oblique angle to, the cell longitudinal axis (Fig. II-7, 18 min arrowheads). Subsequently, transversely oriented MTs began to form on the cell cortex (Fig. II-7, 21-24 min, arrowheads), so that both MTs could be seen to cross on the cell cortex (Fig. II-7, 21-30 min). However, the parallel-oriented MTs had a tendency to disappear so that transverse MTs could be predominantly observed on the cell cortex (Fig. II-7, 51 min), which became typical transverse CMTs. The observations were repeated in a total of 30 randomly chosen cells. Notably, in almost all the independent cells examined, the parallel oriented MTs could be observed and, only after their formation, the transverse MTs could be identified. Thus, in all cases, the formation of parallel-oriented and transversely oriented MTs could be followed in the same cells. It was confirmed in this study, therefore, that the presence of such parallel-oriented MTs is ubiquitous.

Discussions

Significanceof CMT reorganization at the M/G_1 interface

In higher plant cells, the characteristic MT structures of the PPB, the mitotic spindle, phragmoplast and CMTs, appear in sequential order during cell cycle progression. The CMTs are known to control CMF deposition in the same direction as the CMTs. As the "hoops" of CMFs determine the direction of plant cell elongation, the CMTs are thought to play an important role in the morphogenesis of plant cells. The CMTs disappear at the G_2/M interface and reappear after phragmoplast collapse at the M/G_1 interface. Therefore, the study of the mechanism of CMT reorganization is expected to lead to significant contributions to our understanding of plant morphogenesis. I established a BY-GT16 cell line that constitutively expresses a GFP-tubulin fusion protein, and I used this line to time-sequentially observe MT dynamics in living cells. Indeed, using this system, all the MT structures were continuously observed throughout the cell cycle. In the present study, to

reveal the events involving CMT reorganization at the M/G_1 interface, I observed BY-GT16 cells spatially and time-sequentially by deconvolution microscopy or CLSM.

Microscopy for observations and spatial analyses

Deconvolution microscopy consists of a fluorescence microscope with a cooled CCD camera and an attached computer for performing calculations. With this system, figures on different focal planes were first photographed from the cell surface to the mid-plane with adequate intervals, and the data then stored on the computer. Next, by deconvolution calculations performed by the computer, in each figure the fluorescence blur from out-focal planes was mathematically subtracted, and the clear figure on each optical plane then digitally obtained. Finally, the 3D image was constructed by integration of all the figures resulting from the blind deconvolution. By varying the parameters, such as size and brightness of each figure, I could determine the optimal conditions for following the translocation of GFP tubulin at the M/G_1 interface. In contrast, CLSM seems to be highly suited for following phenomena occurring on a fixed focal plane, because CLSM can obtain an optical section of focal plane through pinhole and exclude the signals from out-focal planes. Therefore, in this study, I employed the deconvolution microscopy to spatially analyze tubulin translocation and MT nucleation in whole cell, and the CLSM to perform time-lapse observations of CMT reorganization on the cell cortex.

Migration and recycle of tubulin from phragmoplast

As a result of these analyses using the deconvolution microscopy, the accumulation and translocation of tubulin were observed. At the final stage of phragmoplast collapse, the fluorescence of GFP-tubulin firstly accumulated on the nuclear surface near the cell plate, and then –lagging behind– on the opposite side. When the fluorescence increased on the latter site, it actually decreased on the former, suggesting that tubulin may move between both sides. In addition, the connections of fluorescence were observed between the remnant of the phragmoplast and the first accumulation site. Connections looking like “bridges” were

also observed between both accumulation sites on the nuclear surface. These observations suggest that tubulin may flow and translocate through these connections.

The movement and accumulation of tubulin on the nuclear surface were first observed at the final stage of phragmoplast collapse and never prior to that, suggesting that certain signals may be induced at the initiation of this step. The facts that need to be underlined are that the most bright sites of GFP fluorescence were translocated in order as described above, and that MT nucleation necessarily occurred after the appearance of tubulin accumulation on the nuclear surface opposite the cell plate. Furthermore, the observation that tubulin did not accumulate on the whole nuclear surface but only at several spots or areas, implies that the tubulin did not move by simple diffusion. Taken together, my data suggest that tubulin, a major component of the phragmoplast, was actively transported and recycled as a constituent of nascent MTs. It is uncertain whether de novo synthesized tubulin was involved in nascent MT nucleation or not but, if so, it's contribution is, in view of the observations above and also of the low levels of protein synthesis during mitosis, most probably limited.

CMT reorganization on the cell cortex

I observed the CMT reorganization on the cell cortex of BY-GT16 cells using CLSM, and found that the first CMTs nucleated from the bright spots and elongated parallel to the cell longitudinal axis. Around when the parallel CMTs reached the distal end of the cell, transverse CMTs appeared near the division site, and gradually spread on whole cell cortex. It was proposed previously that at the cell cycle transition from M phase to the G_1 phase, five sequential subphases (I, II, IIIa, IIIb and IIIc) could be observed by immunofluorescence microscopy after staining with anti-tubulin andibodies (Nagata et al. 1994). In particular, after MT organization on the nuclear surface and their elongation to the cell cortex, it was observed that the MTs became transiently parallel to the long axis of the cells. Subsequently, transverse MTs were formed at the site close to the division plane. However, in the previous study, several points remained unresolved, since the process was followed by the frequency

of observed types in a certain population according to the immunofluorescence microscopy. One point concerned whether all the cells, or only a limited fraction of cells, behaved in such a manner. Although the sequential events from I to IIIc have been unequivocally confirmed, the possibility that only some proportion of cells behave in such a manner cannot be excluded. However, this question could be resolved if the fate of a single cell could be followed. Indeed, in more than 30 independent observations, parallel-oriented MTs were, without exception, formed first and then transiently oriented MTs formed. In no case was a reverse of this sequence of events, that is transverse MT formation proceeding parallel MTs, observed. These two kinds of MTs appeared in the different areas of the cell cortex. They seemed to be formed independently, because the CMT distribution changed by the formation of new MTs (Yuan et al. 1994). These results clearly corroborate the previously deduced scheme. Furthermore, it was found that when MTs nucleated from daughter nuclei reached the cell cortex (from I to II), they appeared as the bright spots on the cortex. The CLSM observations revealed that thick bundles of MTs nucleated from the nuclei were certainly connected with these bright spots. We could also follow the rapid MT changes from the appearance of the spots to the organization of the parallel MTs in a single cell.

The bright spots usually appeared after the disruption of phragmoplast. The first CMTs appeared just after the appearance of the bright spots on the cell cortex. The required time, from the appearance of the first CMTs that became the parallel MTs on the cell cortex to the appearance of the transverse MTs, was less than 20 min. The time period, from the appearance of the transverse MTs to their spread throughout the whole cell cortex, was 20-30 min. Therefore, the whole process was completed about within 50 min. This time course was estimated from data with the cells that were 70-80 μm in length, since the long cells had a tendency to have flat surface suitable for the time-sequential observation. The question that therefore arises is why such parallel MTs were formed transiently before the appearance of typical transverse MTs. One possibility may be that such parallel-elongated MTs could provide a measure of cell length. It appears that as soon as the tips of the parallel MTs reach the distal end of cells, the formation of transverse MT begins. Subsequently, at

about the time when the tips of the MTs reached the distal end of the cells, the cell begins to organize transverse MTs at the basal end of the cells. This process is not inconceivable, since similar MTs were assured to be a measure of cell size in fission yeast (Brunner and Nurse 2000). As soon as the tips of MTs reach the distal end of the cells, destruction of MTs will start. Second, the elongation of these MTs could be of some benefit in distributing tubulin precursors throughout the cells. In support of this possibility, the parallel MTs appeared after the disappearance of the phragmoplast, and the transverse MTs spread after the parallel MTs reached the cell end. These observations may also suggest that the tubulin was recycled from the parallel MTs to the transverse MTs after collapse of the phragmoplast. Third, the parallel oriented CMTs might provide the initiation sites of transverse CMTs.

MTOC components on CMT reorganization

Factors involved in MT nucleation and regulation may also be expected to migrate and be recycled through the same path as this tubulin route. In higher plant cells, the nuclear surface was thought to act as a microtubule-organizing center (MTOC) (Vantard et al. 1990, Mizuno 1993, Stoppin et al. 1994, Meier 2001). It has also been reported that the MTOC components, γ-tubulin (Binarová et al. 2000) and Spc98p (Erhardt et al. 2002), were localized on plant nuclei, and were required for MT nucleation. γ-Tubulin was also distributed along all MT arrays (Liu et al. 1993, Joshi and Palevitz 1996, Canaday et al. 2000), whereas Spc98p was localized only at the putative MT nucleation sites on the nuclear surface and the cell cortex (Erhardt et al. 2002). Recently, γ-tubulin was reported to be concentrated only temporarily on the nuclear surface, and to move onto the cell cortex at the M/G_1 interface (Kumagai et al. 2003). Elongation factor 1α (EF-1α), another candidate component of MTOCs, has been implicated in the organization of MTs on the perinuclear region at the M/G_1 interface (Kumagai et al. 1995) and found to be associated with CMTs (Moore and Cyr 2000). Although the localization of Spc98p during mitosis has not yet been investigated, it is likely that components of MTOCs accumulate on the nuclear surface at the M/G_1 interface, and the resulting complex(es) then play an important role in the

nucleation of nascent MTs and the organizations of CMTs on the cell cortex. In fact, γ-tubulin accumulated on the nuclear surface as phragmoplast collapsing, similar to GFP-α-tubulin (Fig. II-5). Noticeably, the γ-tubulin accumulation at the opposite side of the nuclear surface from the cell plate preceded the α-tubulin accumulation (Fig. II-5, g-i). These results may suggest that the accumulation sites of tubulin act as MTOCs, and that MTOC components such as γ-tubulin were necessarily concentrated there. In addition, a hypothesis was recently proposed that new CMT formation initiated on the existing CMTs by branching, where γ-tubulin was localized (Murata et al. 2004). It could be possible that γ-tubulin was transported along the parallel CMTs, and the γ-tubulin on the parallel CMTs acted as a MTOC of newly nucleating transverse CMTs. γ-Tubulin was accumulated on the nuclear surface and then translocated to the cell cortex through the nascent MTs nucleated on the perinuclear region (Fig. II-5, and see Fig. III-6). Therefore, γ-tubulin may be transported along the parallel CMTs from the bright spots to the cell distal ends. This hypothesis could explain why the transverse CMTs firstly appeared near the division plane, and then gradually spread on whole cell cortex. γ-Tubulin might act on the bright spots to nucleate the parallel CMTs and then on the parallel CMTs to initiate the transverse CMTs. Furthermore, some microtubule-associated proteins involved in MT nucleation (Stoppin et al. 1996, Chan et al. 1996) have also been reported to localize on plant nuclei, consistent with the observations of my current study. Moreover, my observation may suggest that MTOC-related proteins are also concentrated once at these sites. For more detailed observations, multi-color labeling with GFP variants for α-tubulin and these MTOC-related proteins is desirable.

Conclusion

In conclusion, detailed process of the CMT reorganization from telophase to early G_1 phase has been clarified for the first time in this study using the unique combination of deconvolution microscopy or CLSM and a BY-GT16 cell line. I hypothesize that the steps involved in CMT reorganization are following. 1) At the final stage of phragmoplast collapse

(Fig. II-8, a), the tubulin moves and accumulates at the nuclear surface near the cell plate (Fig. II-8, b); 2) by flowing through bridges on the nucleus, the tubulin moves to the opposite side of the nucleus (Fig. II-8, c); 3) There, the tubulin accumulates again, and the nascent MTs elongate to the cell cortex (Fig. II-8, d); 4) the bright spots are formed where the nascent MTs reach the cell cortex, and the first parallel oriented CMTs elongate from there (Fig. II-8, e); 5) around when the parallel CMTs reach the distal end of the cell, the transversely oriented CMTs appear near the division site (Fig. II-8, f); 6) as the parallel CMTs disappear, the transverse CMTs spread on whole cell cortex (Fig. II-8, g). The use of the BY-GT16 cell line not only allowed the clear observation of fibrous MTs, but also permitted the spatial and sequential accumulation and movement of free tubulin to be monitored. Although a fusion protein of GFP and the MBD of MAP4 was used to visualize MT structures (Granger and Cyr 2000), the orientation of free tubulin could not be followed because the MBD would not associate with free tubulin, which probably exists as a heterodimer. In turn, however, we could not distinguish whether the putative routes of tubulin on the nuclear surface represented only a flow of free tubulin or also contained fibrous MTs on which free tubulin was transported, possibly using motor proteins. If fibrous MTs and free tubulin could be visualized distinctively in the same cell, new insights are to be expected. A transgenic BY-2 cell line, expressing tubulin and an MBD labeled separately with GFP variants, would be helpful for this purpose. By observing tubulin and MBD simultaneously in the same cell, the processes of free tubulin translocation and MT nucleation could be more clearly demonstrated. More detailed electron-microscopic studies may also be required.

The next question is what regulates the tubulin migration and CMT reorganization at the M/G_1 interface. The distribution of actin cytoskeletons on CMT reorganization will be reported and discussed in the next chapter.

Figures

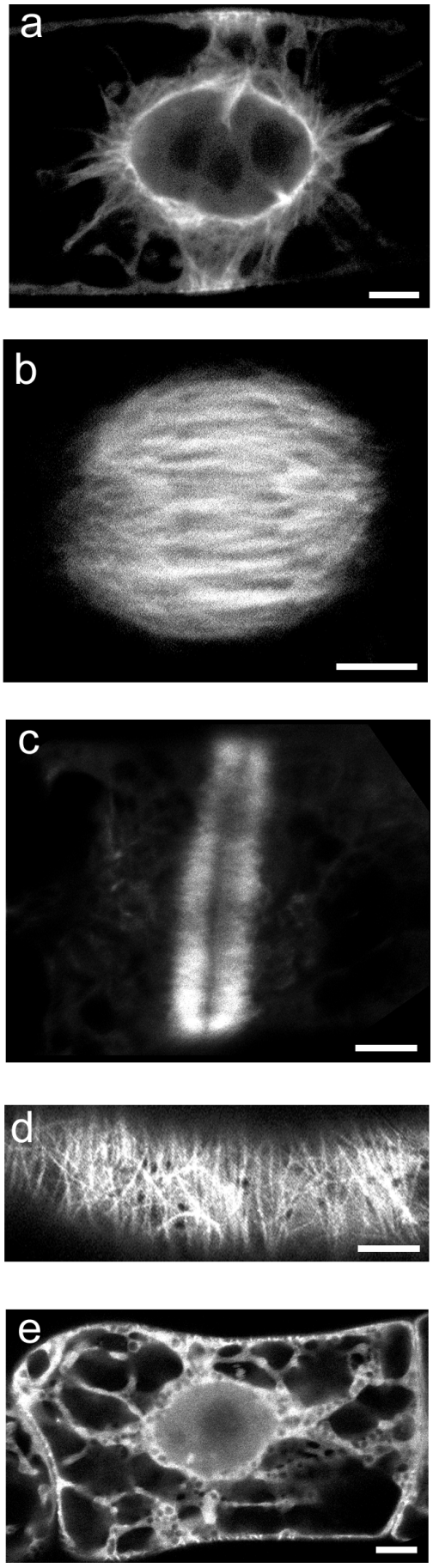

Fig. II-1. Observation of MT structures in BY-GT16 cels by CLSM during cell cycle. In each living cell, the PPB at late G_2 phase (a), the mitotic spindle (b), the phragmoplast at telophase (c), CMTs at G_1 phase (d) and radially-oriented cytoplasmic MTs at S phase (e) were observed in this order. Bars represent 10 μm.

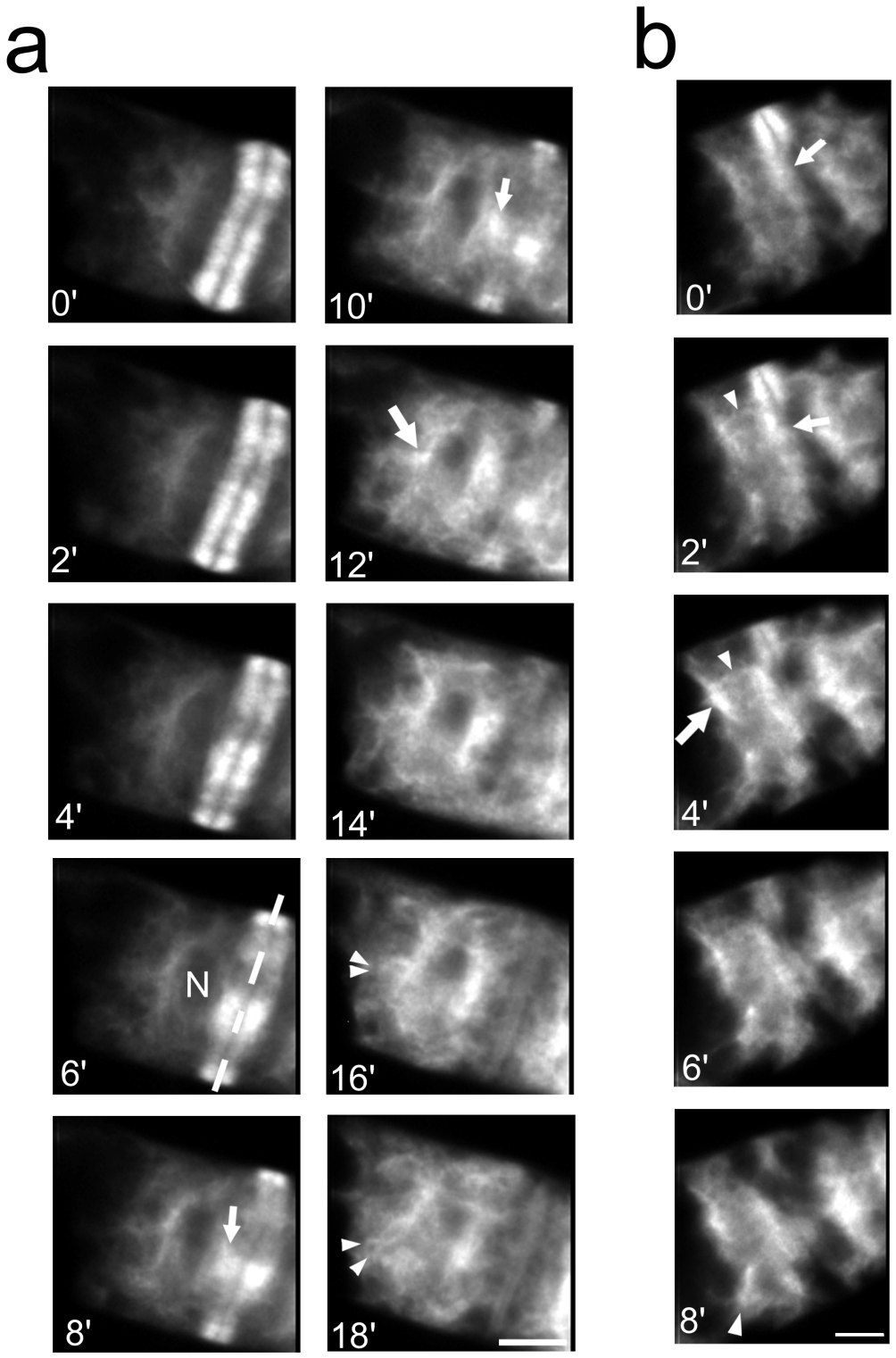

Fig. II-2. Time-sequence observations and spatial analyses at the M/G_1 interface using deconvolution microscopy. (a) At the final stage of phragmoplast collapse, GFP fluorescence accumulated on the nuclear surface near the cell plate (8-10 min, small arrows), followed by accumulation of fluorescence on the other side of nucleus (12 min, large arrow). The MTs that were organized there elongated to the cell cortex (16-18 min, arrowheads). (b) Another BY-GT16 cell observed at right angles to the cell shown in (a). The GFP fluorescence appeared to migrate from the remnant of the phragmoplast and to accumulate on the nuclear envelope near the cell plate (0-2 min, small arrows). Subsequently, the bridge of GFP fluorescence appeared on the nucleus (2-4 min arrowhead), followed by accumulation of GFP fluorescence on the other side of the nucleus (4 min, large arrow). Finally, the nascent MTs elongated to the cell cortex (8 min, arrowhead). Bars represent 10 μm. N, nucleus.

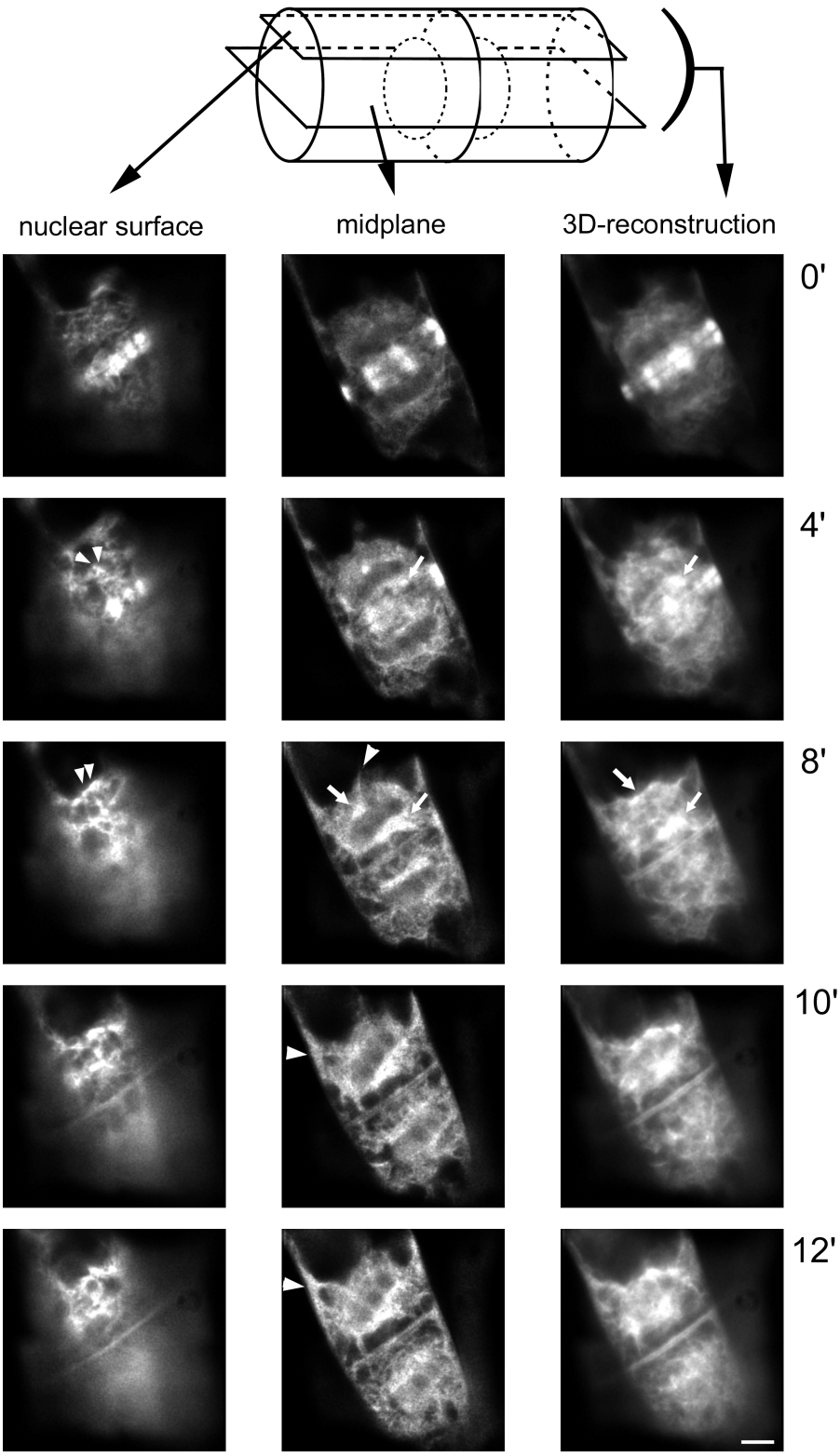

Fig. II-3. Spatial analysis of tubulin migration at the M/G_1 interface. Two focal planes (left, nuclear surface; middle, mid-plane) are shown in addition to the 3D reconstructed images (right). Migrations of GFP fluorescence, from the remnant of the phragmoplast to the nucleus (4-8 min, nuclear surface, small arrowheads), as well as accumulation of fluorescence on the nuclear envelope near the cell plate (4-8 min, mid-plane and 3D, small arrows) were observed. The accumulation on the other side of the nucleus began soon after (8 min, 3D, large arrow), followed by the appearance of the bridges on the nucleus (8 min, nuclear surface, small arrowheads). Nascent cytoplasmic MTs, reorganized from the accumulation sites, were observed (8 min, mid-plane, large arrowhead). Other nascent MTs elongated and reached the cell cortex (10-12 min, mid-plane, large arrowheads). Bar represents 10 μm.

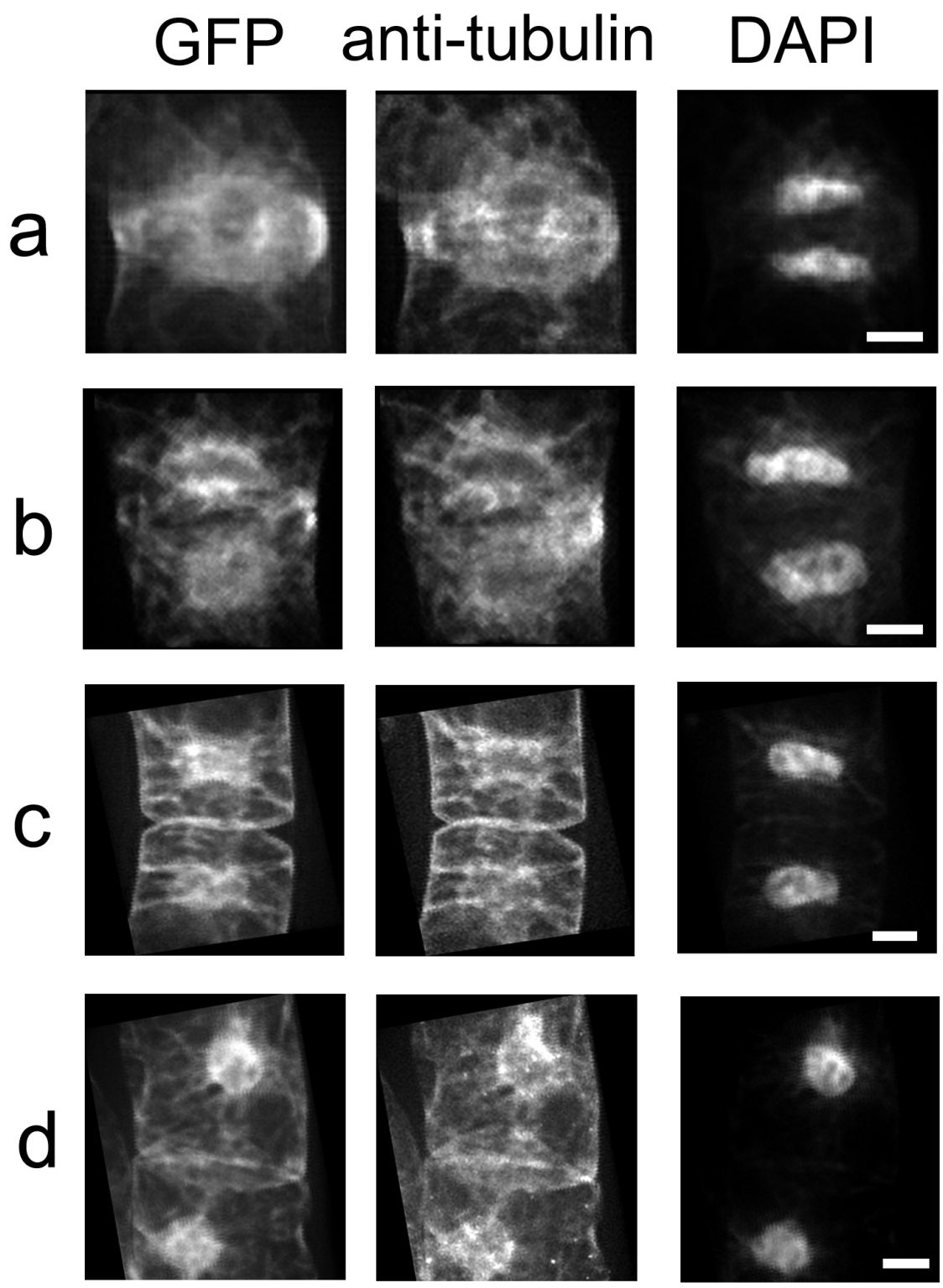

Fig. II-4. Microtubules in BY-GT16 cells at the M/G_1 interface. BY-GT16 cells, stained with anti-tubulin antibodies and rhodamine-conjugated secondary antibody, showing structures with GFP fluorescence (a-d, left column), rhodamine fluorescence (a-d, center column) and DAPI (a-d, right column) by deconvolution microscopy. Remnants of the phragmoplast (a); accumulation of fluorescence on the nuclear surface near the cell plate (b); accumulation at the both sides of the nuclear surface (c); accumulation at the opposite side of the nuclear surface facing away from the cell plate (d). Bars represent 10 μm.

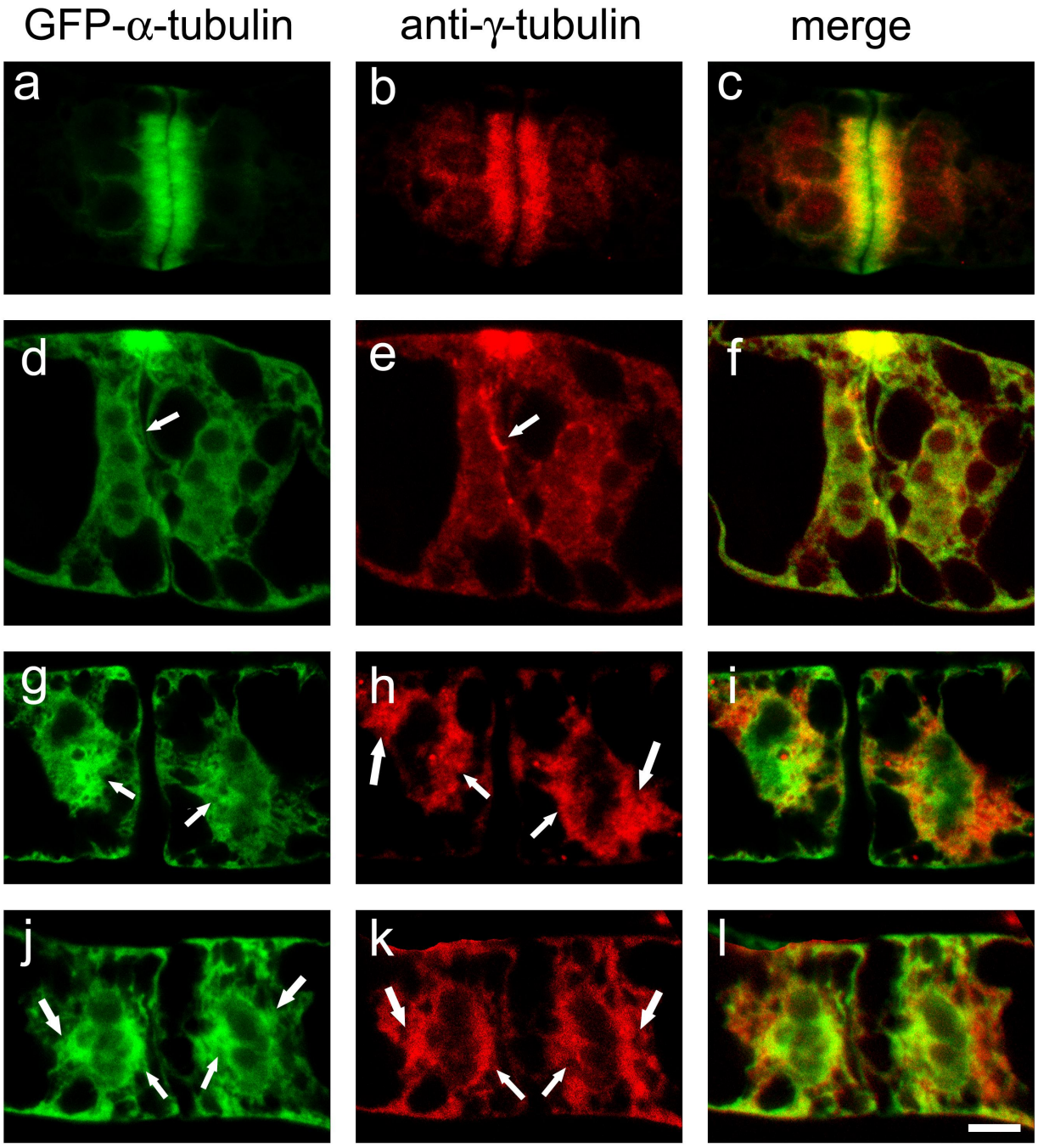

Fig. II-5. Tlanslocation of α-tubulin and γ-tubulin. BY-GT16 cells were stained with anti-γ-tubulin antibody and rhodamine-conjugated secondary antibody. GFP-α-tubulin (a, d, g, j), anti-γ-tubulin (b, e, h, k), and merged images (c, f, i, l) were obtained by CLSM. γ-Tubulin stained the outer sides of phragmoplast MTs (a-c). As phragmoplast collapsing, α-tubulin and γ-tubulin gradually accumulated to the near side of nuclear surface (d-f). When α-tubulin accumulated at the near side (g, arrows), γ-tubulin already accumulated to the opposite side of nuclear surface (h, large arrows). Then, α-tubulin subsequently accumulated to the opposite side, where γ-tubulin had accumulated (j, large arrows). Bar represents 10μm.

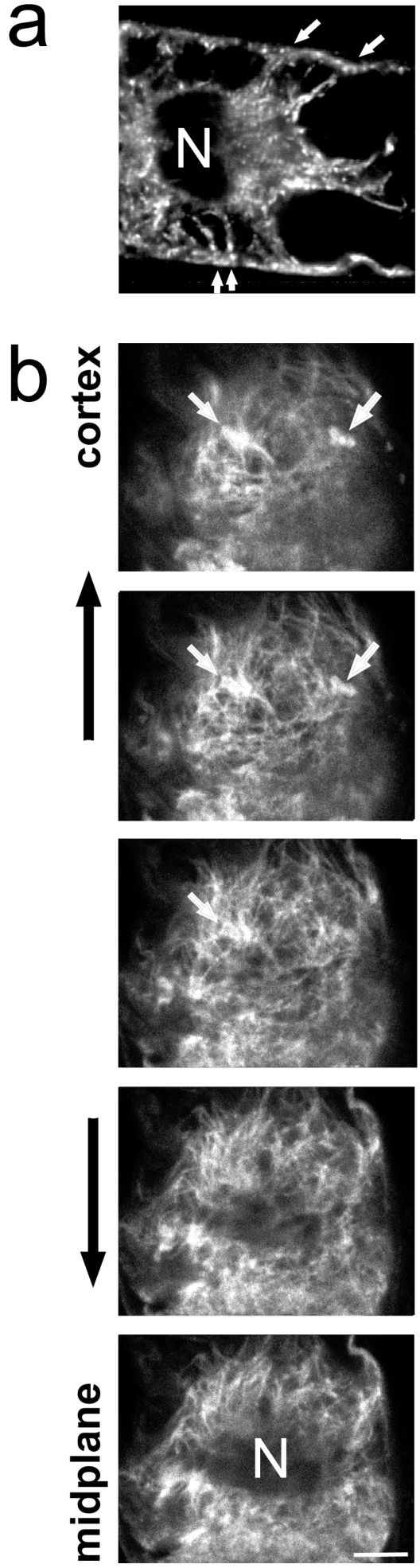

Fig. II-6. Elongation of the nascent MTs from the nuclear surface to the cell cortex. CLSM observations indicate that the thick bundles of MTs (arrows) nucleated from the nucleus reached the cell cortex, were connected with the bright spots on the cell surface. (a) a parallel optical section and (b) transected optical sections of the MTs. Bar represents 10 μm. N, nucleus. Bar represents 10μm.

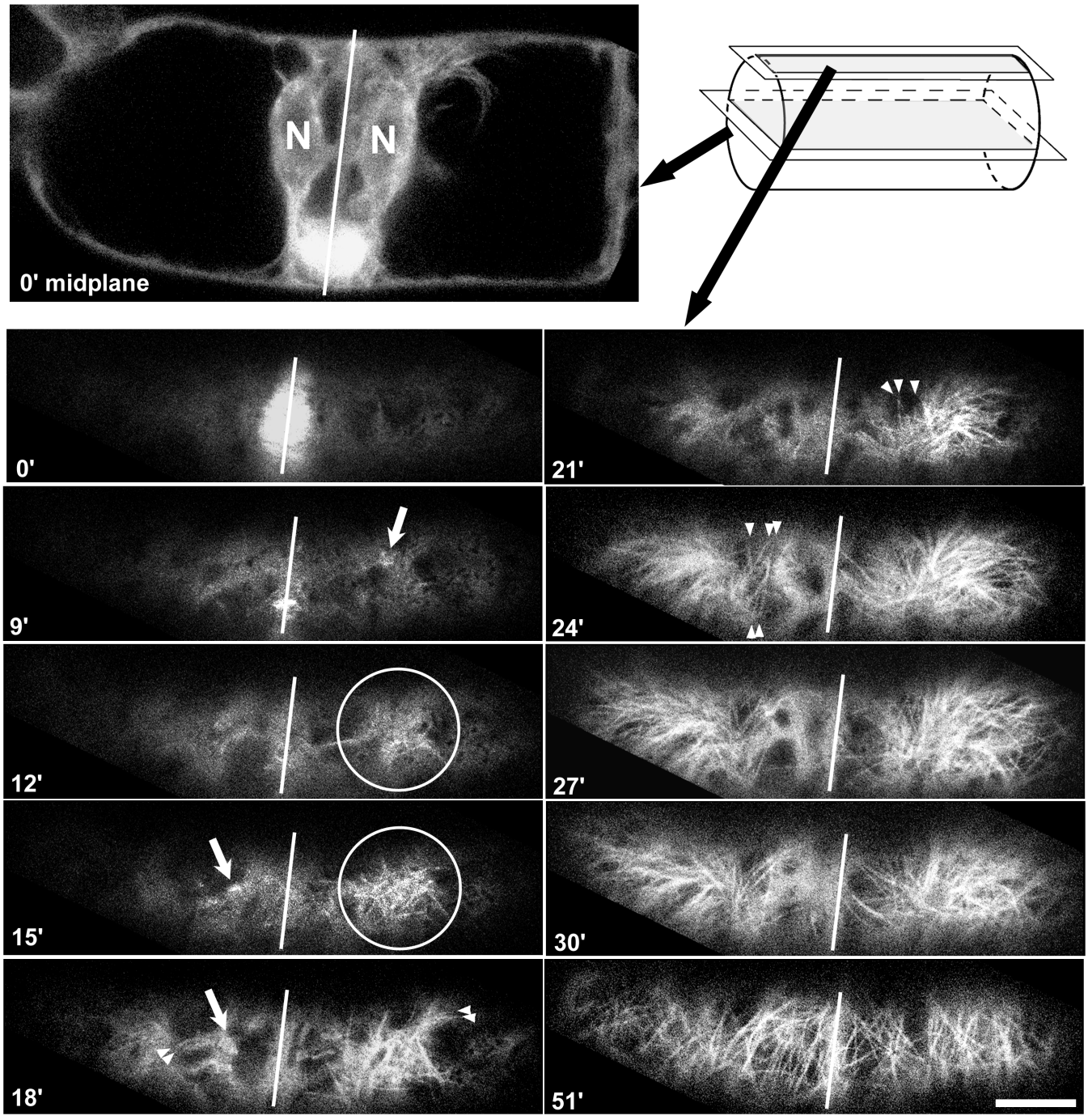

Fig. II-7. Time-sequence observations at the M/G_1 interface. The scans were performed on the cell cortex in a single optical section at 3 min intervals. The reorganization of the CMTs could be observed in detail. 0 min, on both sites of the division plane (line), daughter nuclei (N) were observed with the rest of the phragmoplast. 9-15 min, appearance of the bright spots (arrows) and the randomly oriented short MTs (circle). 18 min, elongation of the parallel MTs (arrowheads). 21-30min, appearance (arrowheads) and spread of transverse MTs. 51 min, spread of transverse CMTs on the whole cell cortex. Bar represents 10 μm.

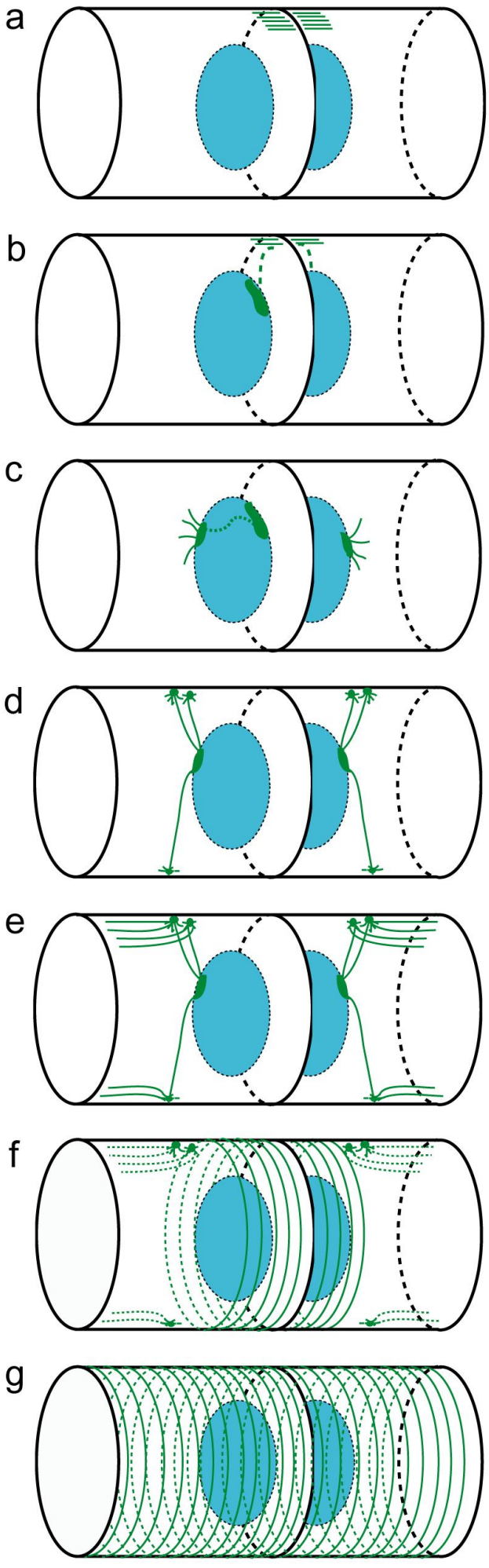

Fig. II-8 Model of CMT reorganization process at the M/G_1 interface. The GFP fluorescence of tubulin and MTs are shown as green, and the nuclei as blue, respectively. The tubulin appears to be transported and recycled in the following order; remnant of phragmoplast (a) → nuclear surface near the cell plate (b) → bridge on the nucleus (c) → nuclear surface opposite the cell plate (c) →nascent MTs (c-d) → bright spots (d) → parallel MTs (e) → transverse MTs (f-g).

Chapter III

Roles of actin microfilaments on cortical microtubules reorganization at the M/G_1 interface

Introduction

Higher plant cells possess four characteristic MT structures: CMTs that regulate the direction of CMF deposition; the PPB that predicts the future division site; the mitotic spindle that segregates the chromosomes; and the phragmoplast that forms the cell plate. A phragmoplast consists of two "anti-parallel" sets of MT arrays on both sides of a mid-zone where MTs are absent. In normal vegetative cells, the phragmoplast is initiated from the interzonal array of MTs between segregated sister chromosomes in anaphase/telophase, and spreads as a ring-like structure that surrounds the leading edge of the cell plate (Verma 2001). Cell plate formation begins with vesicle fusion, following callose and cellulose deposition (Samuels et al. 1995). The vesicles are thought to be transported along phragmoplast MTs (Palevitz and Hepler 1974, Kakimoto and Shibaoka 1988), probably by plus end-directed kinesin-like motor proteins (Asada and Shibaoka 1994, Nishihama et al. 2002).

As well as MTs, actin microfilaments (MFs) are also aligned on the phragmoplast, and form a ring-like structure that surrounds the cell plate (Kakimoto and Shibaoka 1987, Kakimoto and Shibaoka 1988, Cleary et al. 1992, Hasezawa et al. 1998). Although some reports have argued for the involvement of MFs in vesicle transport (Kakimoto and Shibaoka 1988) or in guidance of the cell plate to the correct division site (Kakimoto and Shibaoka 1987, Valster and Hepler 1997, Palevitz and Hepler 1974, Mineyuki and Palevitz 1990), MFs on the phragmoplast appear not to be essential for cell plate formation, since the cell plate can enlarge and join the parental cell wall and cytokinesis can also be completed even when the MFs are disrupted by actin polymerizing inhibitors. Therefore, the functions of MFs on the phragmoplast are still unclear.

The phragmoplast becomes organized in anaphase/telophase, and collapses at the M/G_1

interface. Accompanying phragmoplast collapse, free tubulin protein, released from the phragmoplast, is first translocated to and accumulates on the surface of the daughter nuclei (Chapter II, Yoneda and Hasezawa 2003), followed by MT elongation from the nuclear surface to the cell cortex (Chapter II, Hasezawa et al. 2000, Granger and Cyr 2000, Yoneda and Hasezawa 2003). When the MTs reach the cell cortex, bright spots appear on the cell cortex, from where nascent CMTs parallel to the cell longitudinal axis become elongated, followed by transverse CMT reorganization (Chapter II, Kumagai et al. 2001, Yoneda et al. 2003, Yoneda and Hasezawa 2003). Although these processes from phragmoplast collapse to CMT reorganization have been clarified, the regulatory mechanisms of the process are still unclear.

In this study, I have focused on the roles of MFs and, in particular, on the structural changes of MTs at the M/G_1 interface in the absence of MFs. BY-GT16 cells, transgenic tobacco BY-2 suspension cultured cells stably expressing a GFP-α-tubulin fusion protein, were treated by the actin polymerization inhibitor, Bistheonellide A (BA, Saito et al. 1998), and then time-sequential observations by deconvolution microscopy or CLSM were performed. When the MFs were disrupted by BA treatment, the cells showed no signs of CMT reorganization. Although in about 80 % of the BA-treated cells the tubulin did not move and remained at the site where the phragmoplast had previously existed, we found that in about 20 % of BA-treated cells the tubulin moved irregularly and formed phragmoplast-like structures of MTs in the outer equatorial regions after the original phragmoplast had collapsed. These extra-phragmoplasts had a mono-layered appearance, that is a half of the “anti-parallel” MT set of normal phragmoplasts, but were functionally able to form the extra-cell plates. Furthermore, γ-tubulin, a component of the MTOC, was also localized on the extra-phragmoplast instead of on the cell cortex. Based on these data, I discuss the role of MFs on CMT reorganization and phragmoplast formation.

Materials and Methods

Plant material and synchronization

Suspension cultures of a BY-GT16 (BY-2 cells expressing GFP-tubulin fusion protein clone 16) cell line were maintained as the original tobacco BY-2 cell suspensions (Nagata et al. 1992). Briefly, the BY-GT16 cell suspensions were diluted 95-fold with a modified Linsmaier and Skoog medium at weekly intervals, and agitated on a rotary shaker at 130 rpm at 27 °C in the dark. For cell synchronization, 10 mL of 7-day-old BY-GT16 cells were transferred to 95 mL of fresh medium and cultured for 24 h with 5 mg liter^{-1} aphidicolin (Sigma Chemical Co., St. Louis, MO, U.S.A.). The cells were washed with 10 volumes of the fresh medium and then resuspended in the same medium. The peak of mitotic index of ca. 60 % could be observed at 9.5~10 h after the release from aphidicolin (Chapter I, Kumagai et al. 2001).

Drug treatment

Bistheonellide A (Saito et al. 1998) was dissolved in dimethyl sulfoxide (DMSO) to 1 mM and stored at –20°C. The solution was thawed immediately before use and added to the cell suspension at a final concentration of 1 μM. The treated cell suspension was incubated on a rotary shaker at 130 rpm at 27 °C in the dark.

Time-sequence observations and spatial analysis of BY-GT16 cells using CLSM and deconvolution microscopy

Co-localization of GFP fluorescence and tubulin molecules has been clearly observed in living BY-GT16 cells (Chapter I, Kumagai et al. 2001). For the time-sequence observations, synchronized or 3~4-day-old BY-GT16 cells were transferred into ϕ35 mm Petri dishes with poly-L-lysine-coated ϕ14 mm coverslip windows at the bottom (Matsunami Glass Ind., Ltd., Osaka, Japan). The dishes were placed onto the inverted platform of a fluorescence microscope (IX, Olympus Co. Ltd., Tokyo, Japan) equipped with a confocal laser scanning head system (GB-200, Olympus) or a cooled CCD camera head system (CoolSNAP HQ,

PhotoMetrics Inc., Huntington Beach, Canada). Using the latter system, the Z-stack figures acquired were deconvoluted by AutoDeblur software (AutoQuant Imaging Inc., California, U.S.A.) to digitally display the optical sections, which were then 3D-reconstructed using MetaMorph software (Universal Imaging Co., Downingtown, Panama). Subsequently, the images were digitally processed, using Photoshop software (Adobe Systems Inc., California, U.S.A.).

Immunocytochemistry and cell staining

For the simultaneous observation of MTs and MFs or γ-tubulin, BY-GT16 cells were treated with 250 μM m-maleimidobenzoyl-N-hydroxysuccinimide ester (MBS; Pierce Chemical Co., Rockford, IL, U.S.A.) for 30 min prior to fixation. They were fixed with 3.7 % (w/v) formaldehyde solution for 1 h and then placed onto coverslips coated with poly-L-lysine. The cells were then treated with an enzyme solution containing 0.1 % pectolyase Y23 and 1 % cellulase Y-C (both from Seishin Co., Tokyo, Japan) for 5 min, followed by washing with PMEG solution (50 mM PIPES, 1 mM $MgSO_4$, 5 mM EGTA, and 1 % Glycerol, pH 6.8). Treatment with a detergent solution containing 1 % IGEPAL CA-630 was then performed for 15 min as described in Hasezawa and Nagata (1991), followed by washing with phosphate-buffered saline (PBS; 20 mM Na-phosphate and 150 mM NaCl, pH 7.0). The cells were subsequently treated with a glycine solution (0.1 M glycine, 1 % Bovine Serum Albumin and 0.005 % Triton X-100 in PBS) for 10 min, followed by washing with PBS. To stain γ-tubulin, the cells were incubated with clone G9 antibody (mouse monoclonal antibody raised against *Schizosaccharomyces pombe* γ-tubulin; Kumagai et al. 2003) for 1 h, washed with PBS, and then incubated with a rhodamine-conjugated goat anti-mouse antibody (Cappel Co., West Chester, PA, U.S.A.) for 1 h, followed by washing with PBS. To stain MFs, the cells were incubated with a rhodamine-phalloidin solution (3.3 μM rhodamine-phalloidin (Molecular Probes, Oregon, U.S.A), 100 mM PIPES, 1 mM $MgSO_4$, 2 mM EGTA (pH 6.9), 5 % DMSO, 0.1 % IGEPAL CA-630) for 30 min. After DNA staining with 20 mg $liter^{-1}$ 4',6-diamidino-2-phenylindole (DAPI) for 5 min, the cells were finally embedded in a glycerol

solution containing an antifading reagent (SlowFade Light; Molecular Probes).

For direct observations of MFs without detergent treatment, the BY-GT16 cells were stained with rhodamine-phalloidin (Molecular Probes) by a modified glycerol permeation method (Olyslaegers and Verbelen 1998, Gestel et al. 2001). Briefly, the cells were incubated in actin staining buffer (50mM PIPES, 5mM EGTA, 1mM $MgSO_4$, 1.5% glycerol, 0.15M mannitol, 66nM rhodamine-phalloidin) for 15min, and then placed onto a slide glass and covered with a coverslip. The specimen was observed and photographed under the CLSM described above.

To observe the newly synthesized cell plate, BY-GT16 cells were stained with 0.05 % aniline blue (Biosupplies Australia, Parkville, Victoria, Australia) for 30min. The cells were subsequently observed by CLSM or deconvolution microscopy as described above.

All procedures described above were performed at room temperature.

Results

Localization of MTs and MFs from metaphase to early G_1 phase

To investigate the precise localization of MTs and MTs, the BY-GT16 cells were stained with rhodamine-phalloidin and DAPI, and observed by deconvolution microscopy (Fig. III-1). At metaphase, when MTs formed the mitotic spindle (Fig. III-1, a-1), the MFs were not localized around the spindle and display the actin-depleted zone (ADZ; Fig. III-1, a-2, bracket) that is thought to participate in demarcation of the future division site (Cleary 1995, Hoshino et al. 2003). At early telophase, when the phragmoplast developed, the MFs became co-localized at that site as described previously (Fig. III-1, b, arrows, Hasezawa et al. 1998). As the phragmoplast was gradually collapsing at late telophase, the MFs that were co-localized in the phragmoplast simultaneously began to disappear (Fig. III-1, c, arrows). At the early G_1 phase, at about which time the CMTs became reorganized, the MFs no longer existed at the division site, but ran parallel to the cell longitudinal axis (Fig. III-1, d-2).

For more detailed observations of MFs around the nucleus, I used the glycerol permeabilizing method (Olyslaegers and Verbelen 1998, Gestel et al. 2001). When

phragmoplast was collapsing and GFP-tubulin accumulation began to appear at the nuclear surface (Fig. III-2, a-1, arrows), the MFs were co-localized there (Fig. III-2 a-2, arrows), and elongated to the cell cortex (Fig. III-2 a-2, arrowhead) prior to the MT elongation. The nascent MTs which nucleated from the nuclear surface (Fig. III-2, b-1, arrowhead) seemed to follow the predeveloped MFs (Fig. III-2, b-2, arrowhead).

To investigate the roles of MFs during cell cycle progression from the M phase to G_1 phase, I disrupted the MFs in this period. Bistheonellide A (BA), a dimeric macrolide that inhibits actin polymerization, caused rapid MF disruption within 30 min after application at a final concentration of 1 μM (Hoshino et al. 2003). Although the MFs were completely disrupted by BA treatment at anaphase/telophase (Fig. III-3, b-2), the arrays of phragmoplast MTs showed no disarrangement compared with normal untreated cells (Fig. III-3, a-1, b-1). Even if BA was added at metaphase, when the phragmoplast had not yet become organized, the phragmoplast could still be formed at anaphase/telophase (data not shown).

Effect of BA on CMT reorganization

To examine the roles of MFs on CMT reorganization at the M/G_1 interface, the cell cortex was time-sequentially observed by CLSM (Fig. III-4, cortex). In control cells, the CMTs were completely reorganized within 1 h after the collapse of the phragmoplast (Fig. III-4, a, cortex). However, in BA-treated cells, the CMTs did not appear even by 3 h after the disappearance of the phragmoplast (Fig. III-4, b, c, cortex). To investigate the reason that CMTs were not reorganized, the mid-plane of the cells were simultaneously observed (Fig. III-4, mid-plane). In the control cell, MTs elongated from the nuclear surface to the cell cortex, after which the nucleus gradually moved away from the division plane (Fig. III-4, a, mid-plane). In contrast, in about 80 % of the BA-treated cells, the fluorescence of the GFP-tubulin showed no movement and remained near the division plane (Fig. III-4, b, mid-plane). Nevertheless, in about 20 % of these cells, phragmoplast-like structures could still become organized (Fig. III-4, c, mid-plane, arrow) after collapse of the original

phragmoplast (Fig. III-4, c, mid-plane, arrowheads).

Time-sequential observations of extra-phragmoplast formation

To investigate how such extra-phragmoplasts became organized, I performed detailed time-sequential observations on the mid-plane of the BY-GT16 cells by CLSM. In control cells, the free tubulin that was released from the collapsing phragmoplast became translocated to and accumulated on the nuclear surface (Fig. III-5, Control, 9-18 min), with subsequent MT elongation from the nuclear surface to the cell cortex (Fig. III-5, Control, 27 min, arrow) as reported previously (Chapter II, Kumagai et al. 2001, Yoneda et al. 2003). However, in some BA-treated cells, some short MTs appeared at the final stage of collapse of the original phragmoplast (Fig. III-5, BA, 42 min, arrow). These MTs did not reach the cell cortex, but instead gradually increased in number (Fig. III-5, BA, 60 min, arrow) until they finally formed a phragmoplast-like structure (Fig. III-5, BA, 114 min).

Characterization of extra-phragmoplast

To examine the features of the extra-phragmoplasts, the cells were observed by CLSM in 1 μm steps, and 3-D images were digitally reconstructed from these data (Fig. III-6A). Front view (Fig. III-6A, a-1, b-1) and rotated view (Fig. III-6A, a-2, b-2) images were then examined. In a control cell, the phragmoplast appeared as a well-ordered circular structure, with the mid-region at the site of cell plate formation being depleted of GFP-fluorescence between the bi-layer MTs of the phragmoplast (Fig. III-6A, a-1, a-2). The original phragmoplasts of BA-treated cells were indistinguishable from those of control cells (data not shown). At phragmoplast collapse in control cells, the tubulin proteins were translocated to and accumulated at the nuclear surface, from where the nascent MTs elongated, followed by CMT reorganization on the cell cortex (Chapter II, Kumagai et al. 2001, Yoneda et al. 2003). However, after collapse of the original phragmoplast, some BA-treated cells were found to have organized extra-phragmoplasts (Fig. III-6A, b). These extra-phragmoplasts were organized independently from, and invariably after collapse of, the original

phragmoplasts. Furthermore, the extra-phragmoplasts somehow possessed a disordered MT array, and seemed conspicuously "mono-layered": the depleted fluorescence zone was not observed, and appeared as one side of a normal phragmoplast (Fig. III-6A, b). To examine whether the extra-phragmoplasts could function in forming cell plates, the BY-GT16 cells were stained with 0.05% aniline blue solution and photographed by deconvolution microscopy. In control cells, the cell plates were observed in the mid-zone of the phragmoplasts (Fig. III-6B, a), and they showed centrifugal growth. In BA-treated cells, the extra-phragmoplasts formed extra-cell plates (Fig. III-6B, b, arrows). As a result, three independent cell plates, one formed by the original phragmoplast (Fig. III-6B, b-2, arrowheads) and the others formed by the extra-phragmoplasts (Fig. III-6B, b-2, arrow), could be simultaneously observed. In this case, two extra-phragmoplasts were organized in the two daughter cells; however, in some cases, only one extra-phragmoplast appeared in one daughter cell and resulted in the appearance of only two cell plates (data not shown). In all cases, these extra-cell plates were distorted and incomplete compared to the original ones that had relatively flat and smooth structures (Fig. III-6B, a-2, b-2).

Localization of γ-tubulin

Since MF disruption caused not only CMT reorganization but also extra-phragmoplast formation, it could conceivably also have affected components of the MTOC. To examine this possibility, I stained BY-GT16 cells using an anti-γ-tubulin antibody, and observed the localization of γ-tubulin by CLSM. At telophase, γ-tubulin was localized in the phragmoplast, especially on both outer edges of the phragmoplast MTs (Fig. III-7, a). After phragmoplast collapse, the tubulin translocated to and accumulated on the nuclear surface, first to the proximal sides of the division site, and then to the distal sides where the translocation of γ-tubulin preceded that of α-tubulin (Fig. III-7, b). Later, the γ-tubulin moved to the cell cortex along the MTs that elongated from the nuclear surface (Fig. III-7, c). When the extra-phragmoplasts became organized in BA-treated cells, the γ-tubulin also localized to the extra-phragmoplast (Fig. III-7, d, arrows), but did not reach the cell cortex.

Discussions

Dynamics of MTs and MFs during mitosis

In higher plant cells, the MTs and MFs display dynamic structural changes during cell cycle progression, and play critical roles in multiple aspects of cellular events. Of special interest are the phases of mitosis, in which the MTs act first as a PPB for predicting the future division site at the late G_2 phase to prometaphase, then as a mitotic spindle for segregating the sister chromosomes at metaphase to anaphase, and finally as a phragmoplast for forming the cell plate at telophase to cytokinesis. The MFs surround the MTs at the late G_2 phase, and become involved in PPB maturation (Mineyuki and Palevitz 1990). Accompanied by PPB disappearance and spindle formation, the PPB-like band of MFs are disrupted and the MFs are eliminated from the region where the PPB had existed, forming the ADZ that appears to serve as some sort of signal that guides the cell plate to join the correct site of the parental cell wall (Cleary 1995, Hoshino et al. 2003). When that phragmoplasts are organized at the interface between anaphase and telophase, the MFs co-localize with the phragmoplast MTs (Kakimoto and Shibaoka 1987, Kakimoto and Shibaoka 1988, Cleary et al. 1992, Hasezawa et al. 1998). After phragmoplast collapse at late telophase, the MFs that had co-localized at this site also disappear. Subsequently, the MFs become localized on the cell cortex, and the CMTs reorganize as following the predeveloped cortical MFs (Hasezawa et al. 1998, Kumagai and Hasezawa 2001).

In the traditional MF staining methods, detergents have been used for permeabilizing the plasma membranes. However, the detergent treatments are likely to affect other membranous structures. In order to stain the MFs without any detergent treatments, I employed a modified glycerol permeabilizing method (Olyslaegers and Verbelen 1998, Gestel et al. 2001). When BY-GT16 cells were incubated with the 1.5 % glycerol buffer, rhodamine-phalloidin was easily incorporated into the cells, resulting fine MF fibers to be observed. From the observations by this method, I succeeded in observing the MFs around the daughter nuclei at the M/G_1 interface. In particular, the MFs were localized near the

nuclear surface where tubulin accumulated, and then elongated towards the cell cortex prior to the elongation of the nascent MTs. The MTs nucleated on the perinuclear region seemed to follow the preceding MFs, resulting in the co-localization of MTs and MFs there. These MFs seemed to participate in tubulin translocation and the MT elongation from the daughter nuclei at the M/G_1 interface..

Effect of Bistheonellide A

To identify the roles of MFs throughout this period, I have examined the effects of MF disruption in synchronized BY-GT16 cells using the actin polymerization inhibitor, Bistheonellide A (BA). BA, isolated from the marine sponge *Theonella* sp., is a dimeric macrolide that is found to inhibit polymerizaton of G-actin and to depolymerize F-actin (Saito et al. 1998). Indeed, I found that BA, at concentrations as low as 1 μM, completely disrupted MFs within 30 min of application. For investigation of cytoskeletal phenomena at specific phases of the cell cycle, it is essential that MFs are disrupted as rapidly as possible. It was found that other actin depolymerizing agents, such as cytochalasin B and cytochalasin D, often used in previous studies, require more than two hours to completely disrupt MFs, even at concentrations as high as 100 μM (Hoshino et al. 2003). However, when I used cytochalasins, the lack of CMT reorganization and the extra-phragmoplast formation reported in this study were still observed, although at far lower incidences (data not shown). Therefore, these phenomena can be considered not as artifacts of BA use but rather the consequences of MF disruption.

Roles of MFs on CMT reorganization

In this study, CMTs did not become reorganized at the M/G_1 interface after disruption of MFs by BA treatment. Although CMTs were reorganized within 1 h after phragmoplast collapse in normal cells, the CMTs were not reorganized in BA-treated cells even 3 h after disappearance of the original phragmoplast. This suggests that MFs are indispensable for CMT reorganization. In about 80 % of BA-treated cells, the tubulin remained at the site

where the phragmoplast had existed, suggesting that MFs are required for tubulin translocation from the collapsing phragmoplast to the nuclear surface. In addition, in about 20 % of the MF-disrupted cells, the nascent MTs were nucleated from the nuclear surface, but they did not reach the cell cortex, and formed the extra-phragmoplasts. This suggests that MFs are also required for MT elongation from the nuclear surface of the daughter nucleus to the cell cortex. The MFs may act as a "guide" or a "target" of MT elongation towards the cell cortex. Furthermore, it has been reported that after the MTs reached the cell cortex, the CMTs elongate following the predeveloped MFs on the cell cortex (Hasezawa et al. 1998, Kumagai and Hasezawa 2001), implying that cortical MFs guide the direction of the organizing CMTs. The CMTs were not reorganized when the MFs were disrupted, probably because tubulin released from the collapsing phragmoplast was not translocated to the cell cortex in the absence of MFs, thus resulting in the lack of the source for CMT nucleation. These findings are in support of my hypothesis of tubulin recycling at the M/G_1 interface (Chapter II, Yoneda and Hasezawa 2003). Because of the low level of gene expression at M phase, tubulin recycling may be important in the rapid reorganization of CMTs and in the directional determination of cell elongation. The MFs may therefore play important roles in tubulin recruitment and CMT reorganization at the M/G_1 interface.

MT nucleation on the nuclear surface

In this study, the MTs were nucleated from the nuclear surface, even in BA-treated cells, when the tubulin proteins relocated there. This suggests that the nuclear surface acts as a MTOC, and that this MTOC capability is independent of MFs. Indeed, the nuclear surface of higher plant cells is thought to function as a MTOC site (Vantard et al. 1990, Mizuno 1993, Stoppin et al. 1994, Meier 2001, Baluška et al. 1997), and I have also demonstrated that nascent MTs are nucleated at tubulin accumulation sites on the nuclear surface at the M/G_1 interface (Chapter II, Yoneda and Hasezawa 2003). In addition, γ-tubulin, a component of the MTOC, accumulated on the nuclear surface in non-treated cells, and this accumulation just preceded that of α/β-tubulin, suggesting that γ-tubulin

participates as MTOC component on the nuclear surface at the M/G_1 interface. If the MFs were disrupted, γ-tubulin was not translocated to the cell cortex but probably functioned in extra-phragmoplast organization. Other MTOC components on the nuclear surface, for example, EF-1α (Kumagai et al. 1995) and Spr98p (Erhardt et al. 2002), may show similar localization to γ-tubulin, and may act on MTOC components. Indeed, EF-1α was localized at the MT nucleation site on the nuclear surface (Kumagai et al. 1995). In cases where MTOC components and tubulin proteins accumulated on the nuclear surface, MT nucleation could occur in the absence of MFs.

Extra-phragmoplast formation

Interestingly, when MFs were disrupted by BA treatment, the MTs that were nucleated on the nuclear surface did not reach the cell cortex but rather formed the extra-phragmoplasts. It is possible that, in the absence of MFs, components involved in phragmoplast formation were irregularly localized along the MTs nucleated on the nuclear surface. Kinesin-like proteins, MT-dependent motors, are known to be localized on the phragmoplast, and of these especially KatAp (Liu et al. 1996), KCBP (Bowser and Reddy 1997), and TKRP125 (Asada et al. 1997) are thought to act on phragmoplast formation or expansion. In this context, the extra-phragmoplasts could form extra-cell plates, suggesting that the cytokinesis-specific syntaxin, KNOLLE (Waizenegger et al. 2000, Völker et al. 2001, Muller et al. 2003), kinesin-like motor protein, PAKRP2, which were thought to be involved in vesicle transport on phragmoplast MTs (Lee et al. 2001), and the MAP cascade, which are reportedly necessary for cell plate expansion (Nishihama and Machida 2001, Soyano et al. 2003), may also contribute to the extra-phragmoplasts. In non-treated cells, the MFs were localized on the original phragmoplasts. The MFs may therefore retain these phragmoplast-associated proteins at the original phragmoplast.

The extra-phragmoplasts appeared in a mono-layered form; that is half of the "anti-parallel" phragmoplast MT arrays. In normal mitotic cells, the phragmoplasts appear at the central region of the anaphase spindle, so that the anti-parallel phragmoplast MTs

are thought to be due to the non-kinetochore spindle MTs overlapping between the daughter nuclei (Hepler and Wolniak 1984, Baskin and Cande 1990). Although phragmoplast formation necessarily follows spindle separation in vegetative cells, it is also known that phragmoplasts are organized in the absence of the spindle and nuclear division in reproductive cells (Brown and Lemmon 2001). In cellularization of syncytia, "adventitious phragmoplasts" were formed between neighboring, non-sister as well as sister nuclei (Shimamura et al. 1998, Brown and Lemmon 1988, Brown and Lemmon 2001). Adventitious phragmoplasts were initiated from overlapped MTs of opposing radial MT systems nucleated from two perinuclear areas (Brown and Lemmon 2001), resulting in the anti-parallel MT arrays. These adventitious phragmoplasts are independent of mitotic spindles, although they are necessarily organized between the nuclei as well as mitotic phragmoplasts. However, the extra-phragmoplasts, first identified in this study, did not become organized at the central region of the mitotic spindles or nuclei. This may suggest that if components involved in the phragmoplasts accumulate, then phragmoplast-like structures could be organized without the spindle, the nuclei, or MFs. In addition, the extra-phragmoplasts, found in BA-treated cells, possess a mono-layered structure. This may suggest that the existence of the mitotic spindle or nuclei at both sides of the phragmoplast formation site is necessary to form anti-parallel phragmoplast MT arrays, or that the MFs are important in the formation of the anti-parallel MT structures.

More recently, another extra-phragmoplast formation was reported (Oka et al. 2004). When the activities of 26S proteasome, which is the primary protease of the ubiquitin-mediated proteolytic system that catalyzes the ATP-dependent degradation of ubiquitinated proteins, was inhibited by MG-132 treatment, CMTs were not reorganized after collapsing the original phragmoplast, and extra phragmoplasts developed. The 26S proteasome was localized on the original phragmoplast (Yanagawa et al. 2002), and participate in degradation of phragmoplast-associated proteins, such as TKRP125 (Oka et al. 2004). The localization of 26S proteasome on the original phragmoplast disappeared when MFs were destroyed by BA treatment (data not shown), suggesting that MFs play important

role in gathering 26S proteasome to the phragmoplast. Therefore, it is possible that, when MFs were depolymerized by BA treatment in this study, 26S proteasome dispersed and phragmoplast-associated proteins remained even after collapsing the original phragmoplast, resulting the extra-phragmoplast formation. In addition, the extra phragmoplasts appeared by 26S proteasome inhibition had normal bi-layered anti-parallel MT arrays, while the extra-phragmoplasts formed by MF disorganization in this study had mono-layered "half of anti-parallel" structures (Yoneda et al. 2004, Oka et al. 2004). Double treatment of BA and MG-132 caused the extra-phragmoplasts with "half of anti-parallel" MT structures (data not shown), suggesting that MFs were required for organizing anti-parallel MT arrays of phragmoplasts.

Conclusion

In summary, my observations suggest that MFs are necessary for CMT reorganization at the M/G_1 interface, and are in accordance with the finding that tubulin is translocated from the phragmoplast to the cell cortex (Fig. III-8). This is the first observation that phragmoplasts appear irrespective of the position of the mitotic spindle or nuclei, and that multiple cell plates can be formed in one nuclear division. These findings also suggest that phragmoplasts can be organized independently of the spindle, nuclei, or MFs, if the components involved in phragmoplast formation are able to accumulate. Using this system, the mechanisms involved in phragmoplast formation, for example, the functions of the phragmoplast-associated kinesins, can be investigated in detail.

Figures

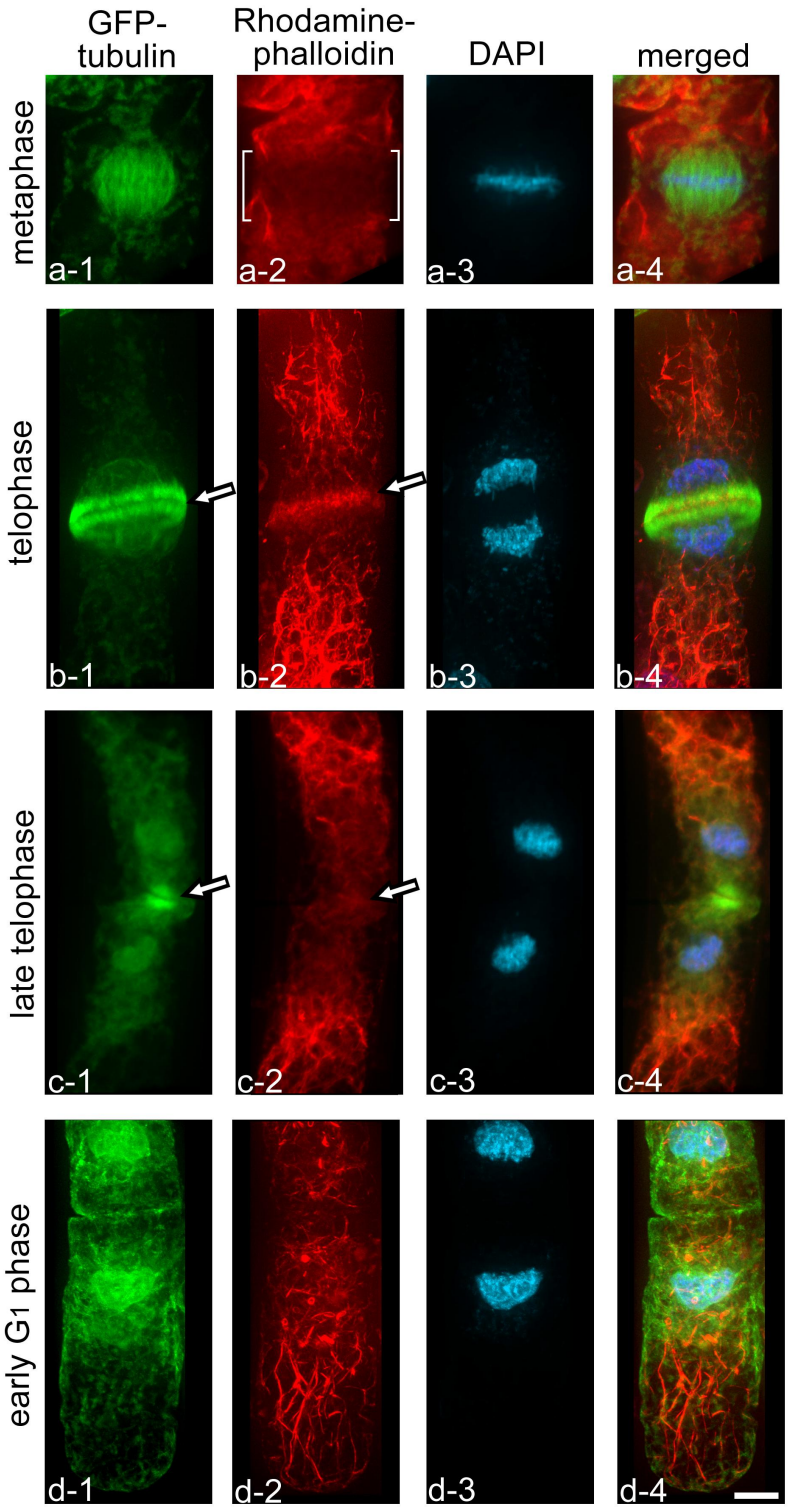

Fig. III-1. Localization of MTs and MFs at the M/G_1 interface. BY-GT16 cells were stained with rhodamine-phalloidin and DAPI. GFP-tubulin (a-1, b-1, c-1, d-1); rhodamine-phalloidin (a-2, b-2, c-2, d-2); DAPI (a-3, b-3, c-3, d-3); and their merged images (a-4, b-4, c-4, d-4) were obtained by deconvolution microscopy. At metaphase, the MTs formed the mitotic spindle (a-1), and the actin depleted zone (ADZ) surrounded it (a-2, bracket). When the phragmoplast appeared at telophase, the MFs co-localized with the phragmoplast MTs, especially in the central region of the phragmoplast (b-1, b-2, arrows). At the collapse of the phragmoplast MTs, the MFs that were co-localized there also disappeared (c-1, c-2, arrows). At the early G_1 phase, the MFs no longer existed near the division site, and ran parallel to the longitudinal axis of the daughter cell (d-2). Bars represent 10 μm.

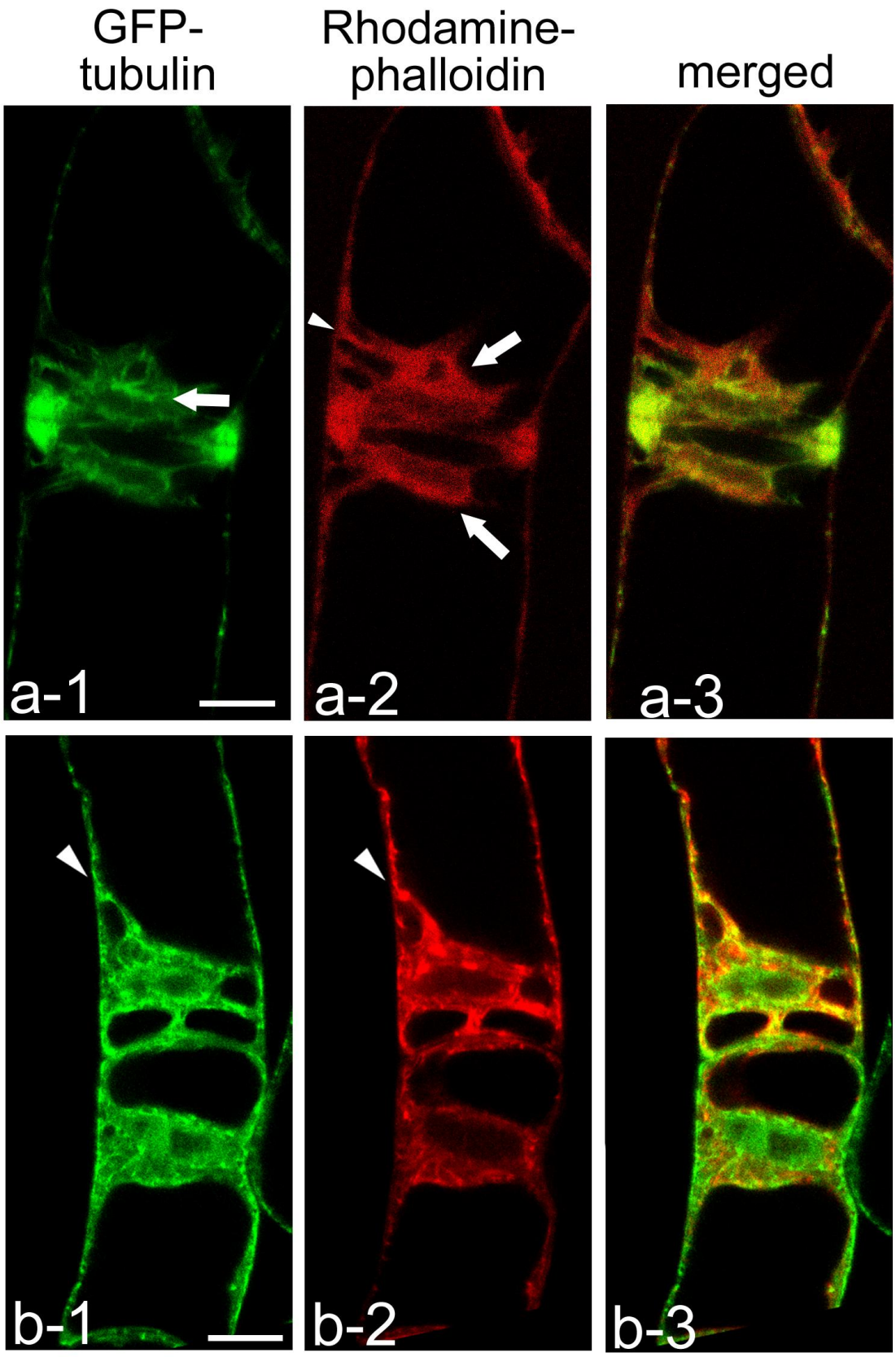

Fig. III-2. Localization of MFs around the daughter nuclei. BY-GT16 cells were stained with rhodamine-phalloidin by glycerol permeabilizing method, and were photographed with CLSM. When phragmoplast was collapsing and GFP-tubulin began to accumulate on the nuclear surface (a-1), MFs already existed there (a-2, arrows), and elongated to the cell cortex (a-2, arrowhead). The nascent MTs which nucleated from the nuclear surface (b-1, arrowhead) were co-localized with MFs (b-2, arrowhead). Bars represent 10 μm.

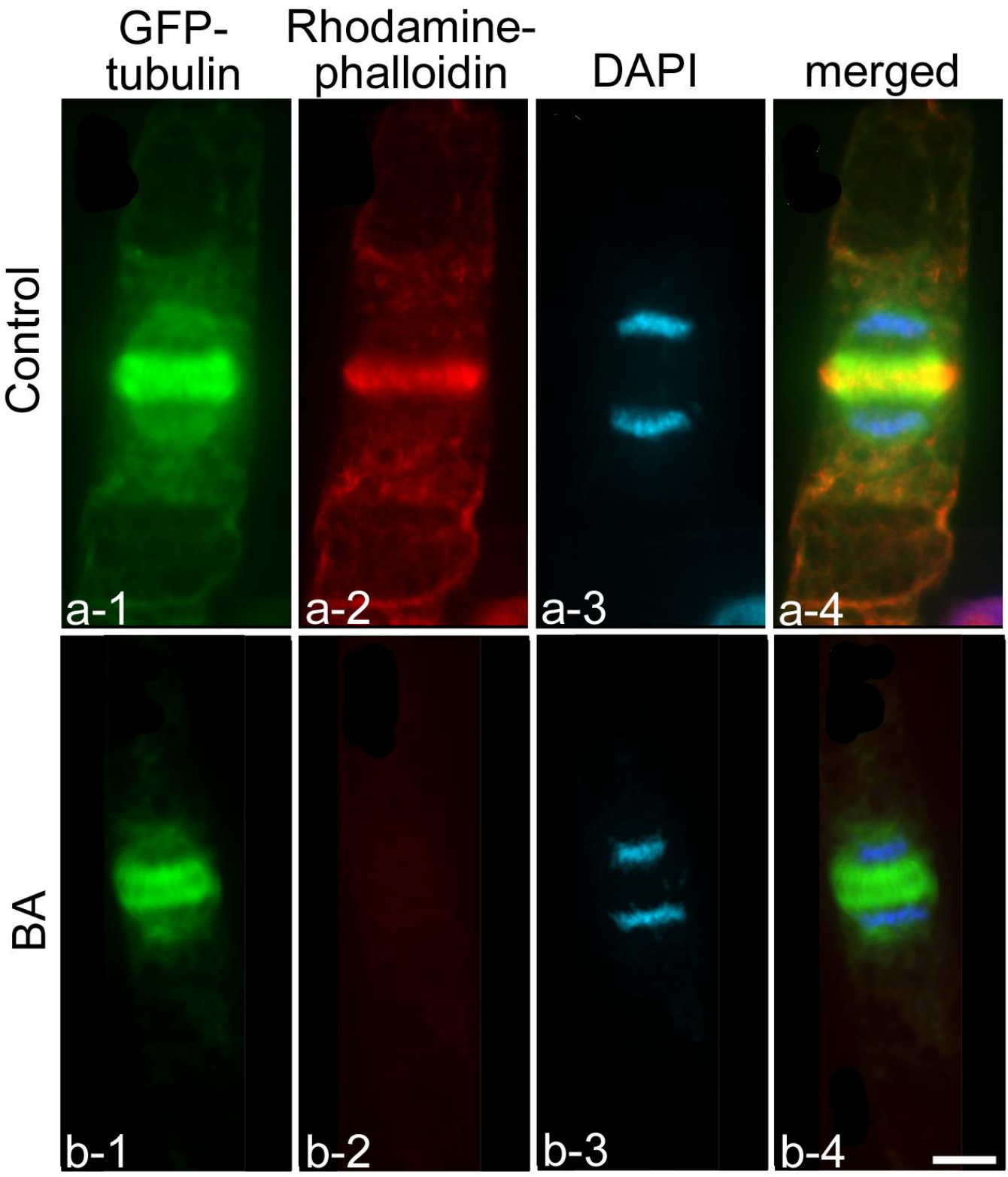

Fig. III-3. Effect of BA. BY-GT16 cells were stained with rhodamine-phalloidin and DAPI. GFP-tubulin (a-1, b-1); rhodamine-phalloidin (a-2, b-2); DAPI (a-3, b-3); and their merged images (a-4, b-4) were obtained by deconvolution microscopy. BY-GT16 cells were treated with BA at a final concentration of 1 μM for 30 min. The MFs were completely disrupted by this treatment (b-2). The images from each fluorescent dye were photographed using the same exposure time and were processed digitally at the same level of correction. Bars represent 10 μm.

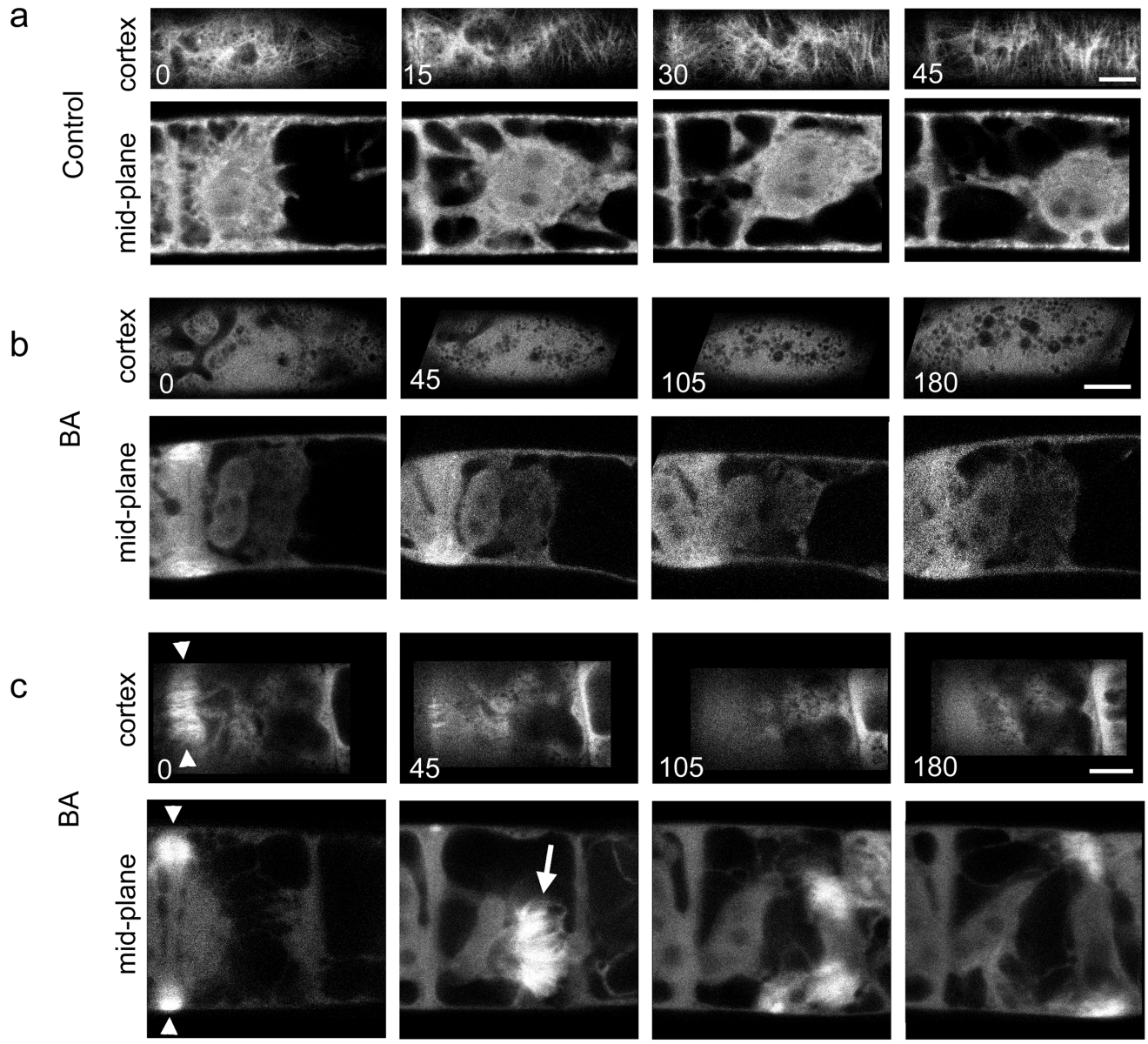

Fig. III-4. Effect of BA treatment on CMT reorganization. The cortex and mid-plane of BY-GT16 cells were simultaneously observed by CLSM at 15-min intervals. In control cells, transverse CMTs were organized within 60 min after the disappearance of the phragmoplast (a, cortex). However, in BA-treated cells, the CMTs were not reorganized even 3 h after phragmoplast collapse (b, c, cortex). In contrast, in about 80 % of the BA-treated cells, fluorescence from the GFP-tubulin did not move and remained at the division plane (b, mid-plane), whereas in about 20 % of these cells, phragmoplast-like structures were organized (c, mid-plane, arrow) after collapse of the original phragmoplasts (c, arrowheads). Bars represent 10 μm.

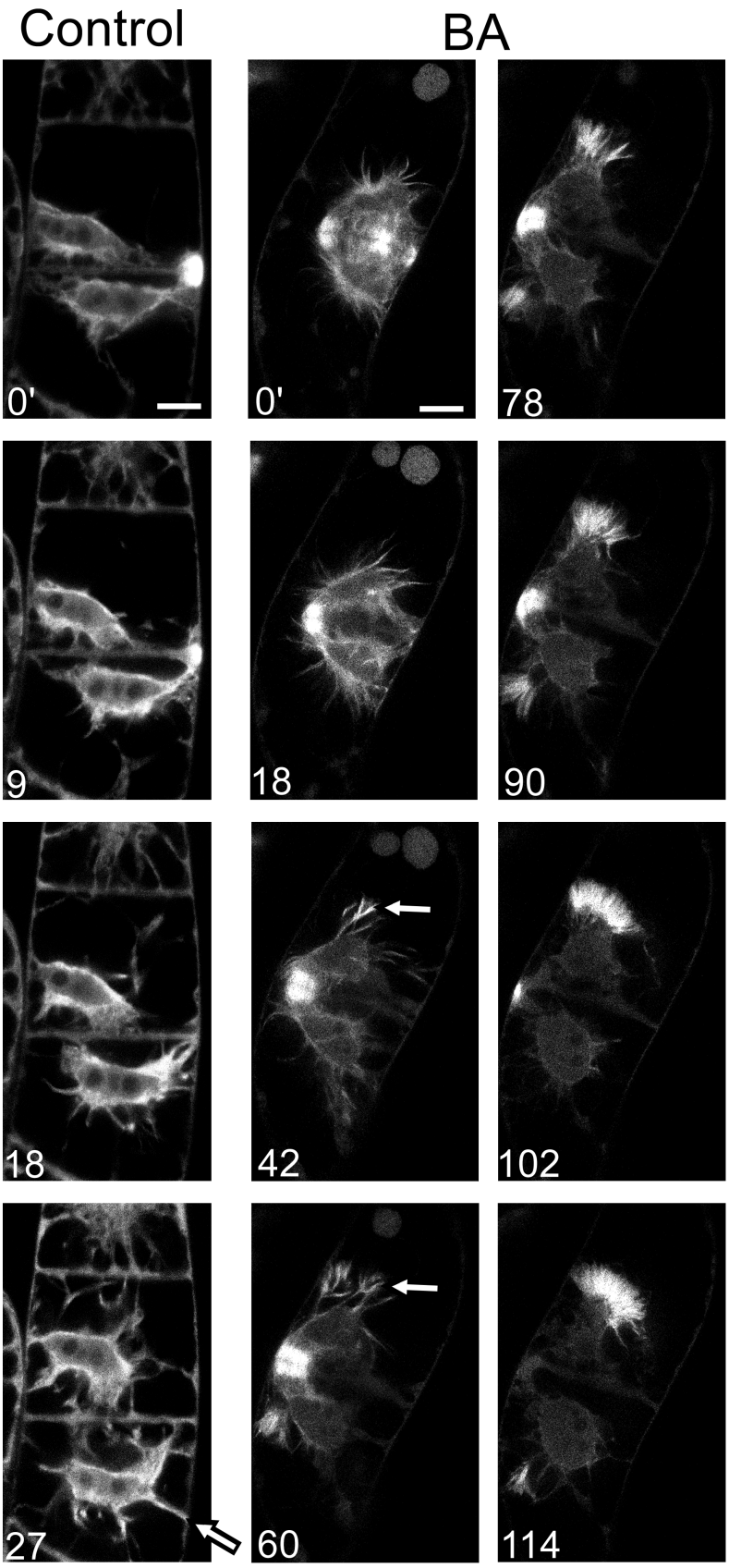

Fig. III-5. Time-lapse observations of extra-phragmoplast formation. BY-GT16 cells were time-sequentially observed by CLSM at 3-min intervals. In control BY-GT16 cells, tubulin proteins released from the collapsing phragmoplast were translocated to the nuclear surface (control, 9-18 min), from where MTs elongated to the cell cortex (Control, 27 min, arrow). In BA-treated BY-GT16 cells, as the original phragmoplast collapsed, the MTs became organized near the nuclear surface (BA, 42-60 min, arrows), and gradually formed a phragmoplast-like structure (BA, 78-114 min). Bars represnet 10 μm.

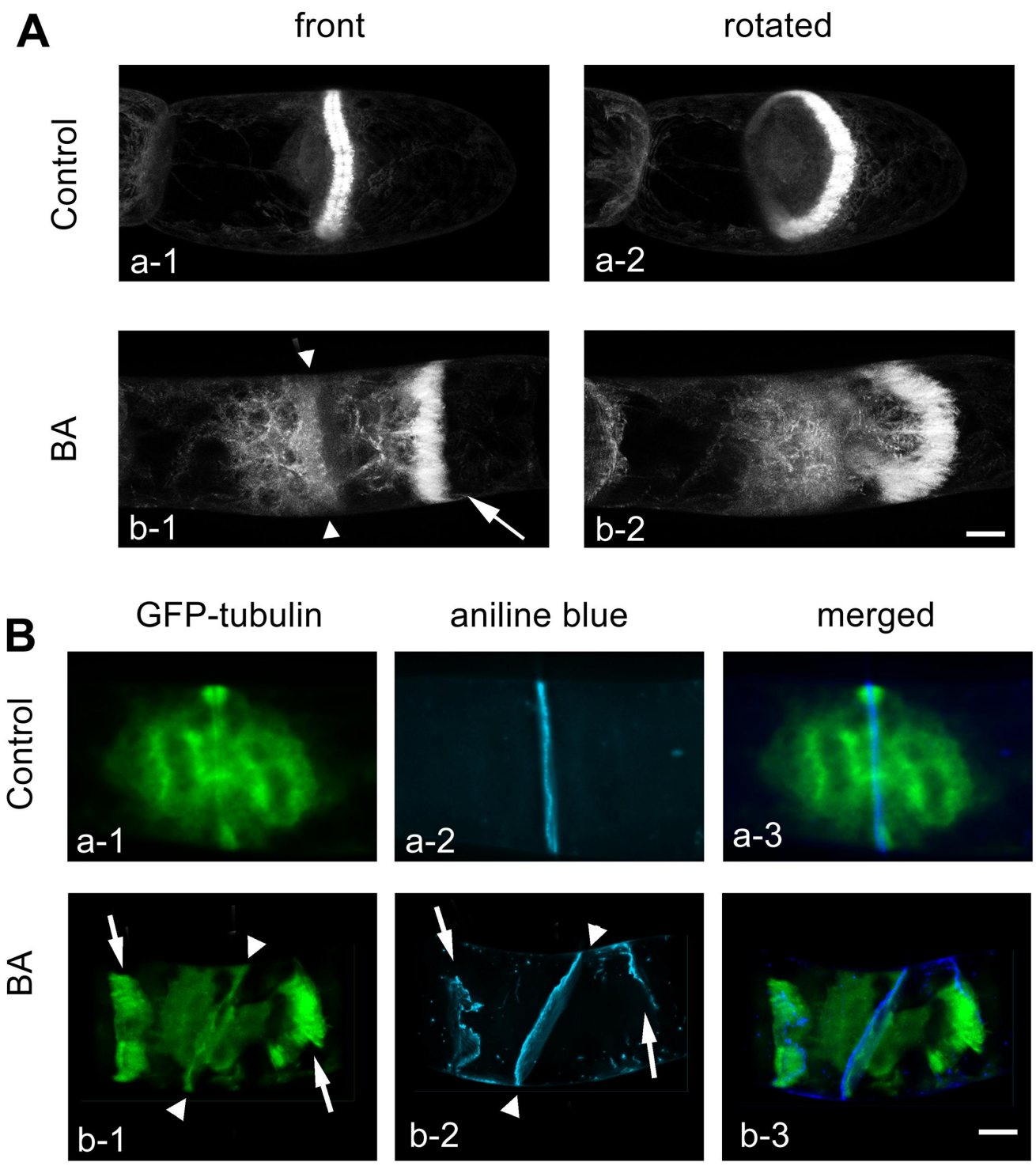

Fig. III-6. Features of the extra-phragmoplast by BA treatment. A) Each focal plane was obtained by CLSM every 1 μm. The data were digitally processed to reconstruct 3-D images, that are presented in front view (a-1, b-1) and rotated view (a-2, b-2). Control cells had circular and bi-layered phragmoplasts (a-1, a-2). When BA was applied at metaphase/telophase, an extra-phragmoplast appeared after collapse of the original phragmoplast (b-1, b-2). The extra-phragmoplast appeared disordered and in a mono-layered form. B) BY-GT16 cells were stained with 0.05 % aniline blue solution and then photographed by deconvolution microscopy. GFP-tubulin (a-1, b-1), aniline blue (a-2, b-2), and their merged images (a-3, b-3) are shown. In the control cell, a flat cell plate was formed (a-2). In the BA-treated cell, extra-phragmoplasts (b-1, arrows) formed extra-cell plates with somewhat distorted structures (b-2, arrows). Arrowheads indicate the original division plane. Bars represent 10 μm.

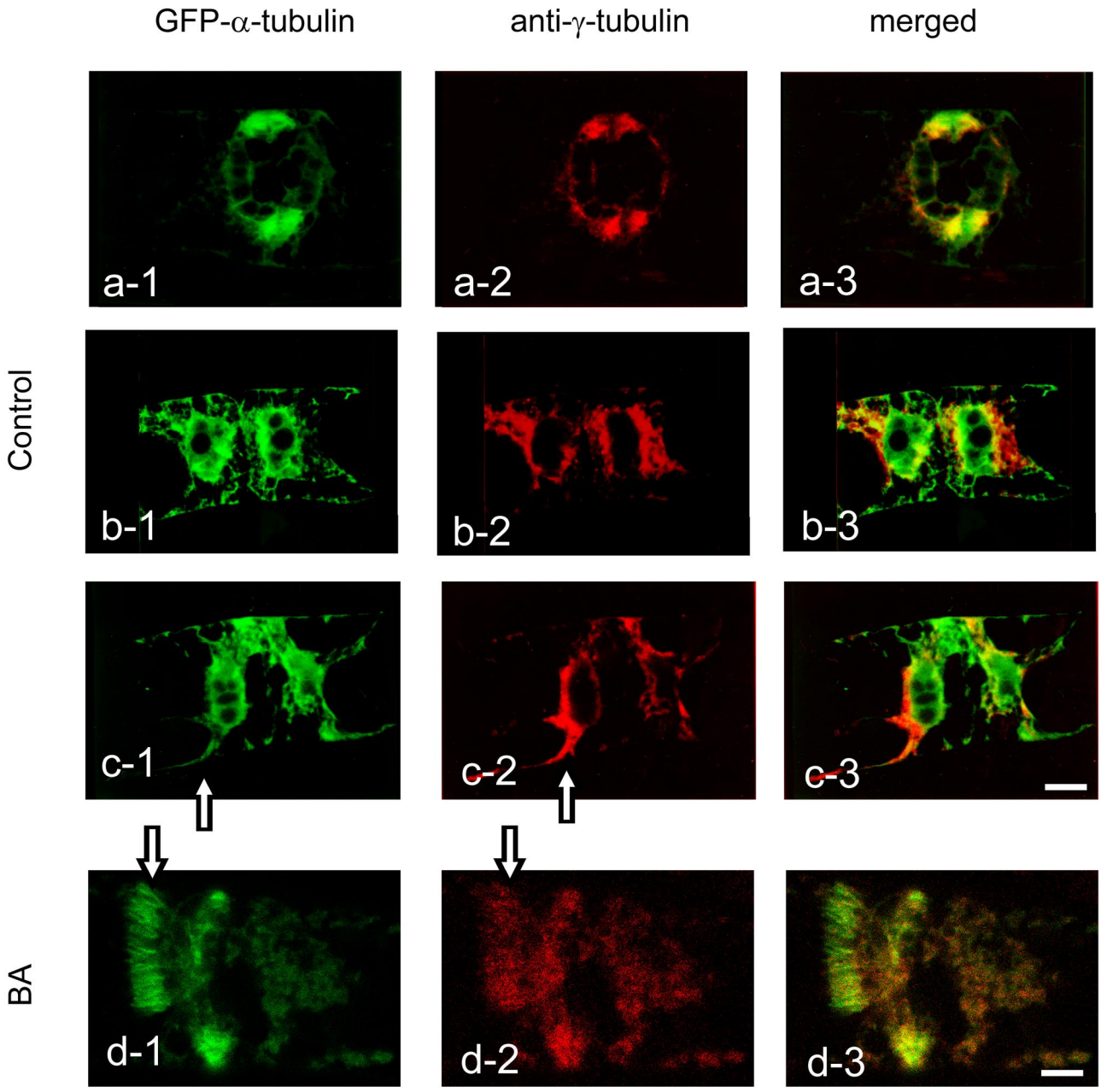

Fig. III-7. Localization of γ-tubulin on the original- and extra-phragmoplasts. BY-GT16 cells were stained with anti- γ-tubulin antibody and rhodamine-conjugated secondary antibody. GFP-α-tubulin (a-1, b-1, c-1, d-1), anti- γ-tubulin (a-2, b-2, c-2, d-2), and their merged images (a-3, b-3, c-3, d-3) were obtained by CLSM. The γ-tubulin stained the outer edges of phragmoplast MTs (a-1, a-2, a-3). As the phragmoplast collapsed, the α-tubulin and γ-tubulin were translocated to the nuclear surface (b-1, b-2, b-3). The γ-tubulin then moved to the cell cortex along the MTs nucleated from the nuclear surface (c-1, c-2, c-3, arrows). When BA was applied and an extra-phragmoplast was organized, the γ-tubulin co-localized there (d-1, d-2, d-3, arrow). Bars represent 10 μm.

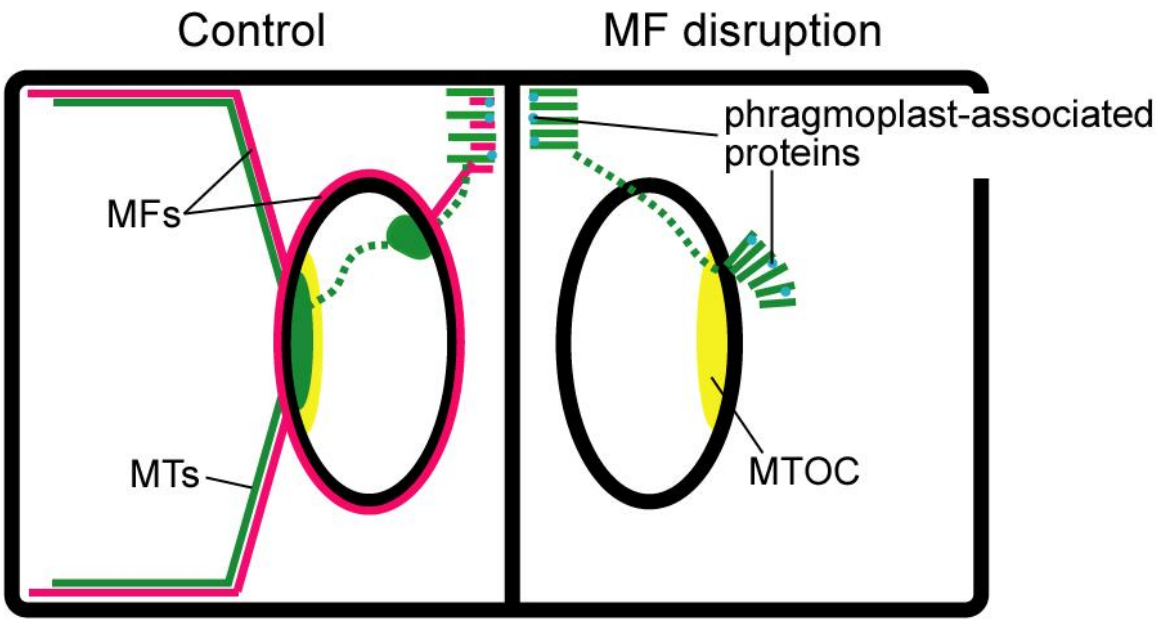

Fig. III-8. A scheme of MF-dependent tubulin recruitment. MTs involving tubulins, MFs, MTOC sites, and putative phragmoplast-associated proteins are shown in green, red, yellow, and blue, respectively. Tubulins, released from the collapsing phragmoplast, translocates to the nuclear surface, and nascent MTs elongate, from the MTOC site on the nuclear surface far away from the division site, to the cell cortex with the guide of MFs (Control). In the absence of MFs, the tubulin transferred to the nuclear surface organizes an extra-phragmoplast, probably with the aid of phragmoplast-associated proteins that are inadequately translocated.

Conclusions and Prospects

To reveal the MT dynamics in living plant cells, I have transformed tobacco BY-2 cell line and established a transgenic BY-2 cell line stably expressing a GFP-tubulin fusion protein clone 16 (BY-GT16). The BY-GT16 cells were indistinguishable from the original BY-2 cells in shape and size, and could be highly synchronized by aphidicolin treatment as the original BY-2 cells. The GFP-fluorescence of BY-GT16 represented all the MT structures correctly during the cell cycle, and the MT rearrangements were time-sequentially observed in the living BY-GT16 cells under the fluorescence microscopy. Therefore, BY-GT16 became a powerful tool for time-lapse observations of MT dynamics in detail.

In order to analyze the phenomena on the CMT reorganization at the M/G_1 interface, I employed two kinds of microscopy: deconvolution microscopy which was suitable for time-lapse observation and spatial analysis, and CLSM which was suitable for obtaining images on a fixed optical plane. When the BY-GT16 cells were spatially and time-sequentially monitored by the deconvolution microscopy, GFP-tubulin was found to accumulate onto the nuclear surface near the cell plate at the final stage of phragmoplast collapse. Subsequently, GFP-tubulin accumulated again on the nuclear surface opposite the division plane, where the nascent MTs elongated to the cell cortex. The use of the BY-GT16 cell line not only allowed the observation of fibrous MTs, but also of free tubulin to be monitored. From these observations, I hypothesized that tubulin which released from the collapsing phragmoplast was actively transported and recycled as a constituent of the reorganizing CMTs. When the CLSM was used to gain the optical section from the cells, the bright spots were formed where the MTs from the perinuclear region reached the cell cortex, and the first CMTs rapidly elongated parallel to the cell longitudinal axis from the bright spots towards the distal end of the cells. Around the time when the tips of the parallel CMTs reached the distal end, the formation of transverse CMTs followed in the cortex near the division site, and then spread through the whole cell cortex, while the parallel MTs disappeared. The whole processes in the mode of CMT reorganization at the M/G_1 interface were clarified in detail.

I also investigated the roles of MFs in the reorganization of CMTs at the M/G_1 interface. When actin microfilaments (MFs) were disrupted by the MF-disrupting agent, bistheonellide A (BA), tubulin translocation and CMT reorganization did not occur even 3 h after phragmoplast collapse, whereas non-treated cells completed CMT reorganization within 1h. In the absent of MFs, the tubulin proteins did not show appropriate recruitment but remained at the site where the phragmoplast had existed. Interestingly, some populations of BA-treated cells formed extra-phragmoplast instead of CMTs. These extra-phragmoplasts could functionally form extra-cell plates. This is the first observation of the formation of multiple cell plates during one nuclear division, and of phragmoplast generation irrespective of the position of the mitotic spindle or nuclei. These results indicated that MFs are necessary for CMT reorganization at the M/G_1 interface, and supported my hypothesis of tubulin recruitment on the mode of CMT reorganization. Furthermore, it was also suggested that the localization of phragmoplast-associated proteins such as kinesins was controlled by MFs.

I am interested in how MFs regulate the CMT reorganization. Especially, localization and interaction of MTs and MFs should be revealed. If visualization of MTs and MFs in single living cell using GFP variants such as YFP (Nagai et al. 2002), DsRed (Dietrich and Maiss 2002), mRFP (Campbell et al. 2002) and HcRed (Fradkov et al. 2002) could be possible, the time-sequential and spatial observations would be clarified the relationship between MTs and MFs at the M/G_1 interface in more detail.

The further interest is that how CMTs, reorganized at the M/G_1 interface, regulate the direction of the following CMF deposition and cell elongation. It is known that the ordered CMTs affect the patterns of CMF deposition on the plant cell surface by controlling the movement of cellulose-synthesizing complexes within the fluid mosaic membrane, and that the deposition patterns of newly-synthesized CMFs determine cell shape (Baskin 2001). The cells become a half in sized after symmetric cell division, and therefore the determination of cell elongation after mitosis is very important process in plant cell morphogenesis. However, it is uncertain whether the cellulose-synthesizing complex is connected directly or regulated

indirectly with CMTs. Recently, several enzymes involved in cellulose biosynthesis have been characterized (Pear et al. 1996, Hazen et al. 2002, Burn et al. 2002, Samuga and Joshi 2002, Beeckman et al. 2002, Zhong et al. 2003, Doblin et al. 2003). The relationship between CMTs and the cellulose-synthesizing complexes could be clarified by observing both structures in living plant cells.-

References

An, G. (1985) High efficiency transformation of cultured tobacco cells. Plant Physiol. 79: 568-570

Asada, T. and Shibaoka, H. (1994) Isolation of polypeptides with microtubule-translocating activity from phragmoplasts of tobacco BY-2 cells. J. Cell Sci. 107: 2249-2257

Asada, T., Kuriyama, R. and Shibaoka, H. (1997) TKRP125, a kinesin-related protein involved in the centrosome-independent organization of the cytokinetic apparatus in tobacco BY-2 cells. J. Cell Sci. 110: 179-189

Baluška, F., Volkmann, D. and Bariow, P.W. (1997) Nuclear components with microtubule-organizing properties in multicellular eukaryotes: Functional and evolutionary considerations. Int. Rev. Cytol. 175: 91-135

Baskin, T.I. and Cande, W.Z. (1990) The structure and function of the mitotic spindle in flowering plants. Annu. Rev. Plant Physiol. Plant Mol. Biol. 41: 277-315

Baskin, T.I. (2001) On the aligment of cellulose microfibrils by cortical microtubules: a review and a model. Protoplasma 215: 150-171

Beeckman, T., Przemeck, G.K.H., Stamatiou, G., Lau, R., Terryn, N., Rycke, R.D., Inzé, D. and Berleth, T. (2002) Genetic complexity of cellulose synthase A gene function in Arabidopsis embryogenesis. Plant Physiol. 130: 1883-1893

Binarová, P., Cenklová, V., Hause, B., Kubátová, E., Lysák, M., Doležel, J., Bögre, L. and Dráber, P. (2000) Nuclear γ-tubulin during acentriolar plant mitosis. Plant Cell 12: 433-442

Bowser, J. and Reddy, A.S.N. (1997) Localization of a kinesin-like calmodulin-binding protein in dividing cells of *Arabidopsis* and tobacco. Plant J. 12: 1429-1437

Brown, R.C. and Lemmon, B.E. (1988) Cytokinesis occurs at boundaries of domains delimited by nuclear-based microtubules in sporocytes of *Conocephalum conicum* (Bryophyta). Cell Motil. Cytoskeleton 11: 139-146

Brown, R.C. and Lemmon, B.E. (2001) Phragmoplasts in the absence of nuclear division. J. Plant Growth Regul. 20: 151-161

Brunner, D. and Nurse, P. (2000) Clip 170-like tip1p spatialy organized microtubular dynamics in fission yeast. Cell 112: 695-704

Burn, J.E., Hocart, C.H., Birch, R.J., Cork, A.C. and Williamson, R.E. (2002) Functional Analysis of the Cellulose Synthase Genes *CesA1, CesA2, and CesA3* in Arabidopsis. Plant Physiol. 129: 797-807

Campbell, R.E., Tour, O., Palmer, A.E., Steinbach, P.A., Baird, G.S. and Zacharias, D.A. (2002) A monomeric red fluorescent protein. Proc. Natl. Acad. Sci. U.S.A. 99: 7877-7882

Canaday, J., Stoppin-Mellet, V., Mutierer, J. and Lambert, A.M. (2000) Higher plant cells: gamma-tubulin and microtubule nucleation in the absence of centrosomes. Microsc. Res. Tech. 49: 487-495

Chan, J., Rutten, T. and Lloyd, C. (1996) Isolation of microtubule-associated proteins from carrot cytoskeletons: a 120 kDa map decorates all four microtubule arrays and the nucleus. Plant J. 10: 251-259

Cleary, A.L., Gunning, B.E.S., Wasteneys, G.O. and Hepler, P.K. (1992) Microtubule and F-action dynamics at the division site in living *Tradescantia* stamen hair cells. J. Cell Sci. 103: 977-988

Cleary, A.L. (1995) F-actin redistributions at the division site in living *Tradescantia* stomatal complexes as revealed by microinjection of rhodamine-phalloidin. Protoplasma 185: 152-165

Dietrich, C. and Maiss, E. (2002) Red fluorescent protein DsRed from Discosoma sp. as a reporter protein in higher plants. BioTechniques 32: 286-291

Doblin, M.S., Kurek, I., Jacob-Wilk, D. and Delmer, D.P. (2003) Cellulose biosynthesis in plants: from genes to rosettes. Plant Cell Physiol. 43: 1407-1420

Erhardt, M., Stoppin-Mellet, V., Campagne, S., Canaday, J., Mutterer, J., Fabian, T., Sauter, M., Muller, T., Peter, C., Lambert, A.M. and Shimit, A.C. (2002) The plant SPC98p homologue colocalizes with γ-tubulin at microtubule nucleation sites and is required for microtubule nucleation. J. Cell Sci. 115: 2423-2431

Fradkov, A.F., Verkhusha, V.V., Staroverov, D.B., Bulina, M.E., Yanushevich, Y.G.,

Martynov, V.I., Lukyanov, S. and Lukyanov, K.A. (2002) Far-red fluorescent tag for protein labelling. Biochem. J. 368: 17-21

Gestel, K.V., Le, J. and Verbelen, J.P. (2001) A comparison of F-actin labeling methods for light microscopy in different plant specimens: multiple techniques supplement each other. Micron 32: 571-578

Goddard, R.H., Wick, S.M., Silflow, C.D. and Snustad, D.P. (1994) Microtubule components of the plant cell cytoskeleton. Plant Physiol. 104: 1-6

Granger, C.L. and Cyr, R.J. (2000) Microtubule reorganization in tobacco BY-2 cells stably expressing GFP-MBD. Planta 210: 502-509

Gunning, B.E.S. and Hardham, A.R. (1982) Microtubules. Annu. Rev. Plant Physiol. 33: 651-698

Hasezawa, S. and Nagata, T. (1991) Dynamic organization of plant microtubules at the three distinct transition points during the cell cycle progression of synchronized tobacco BY-2 cells. Bot. Acta 104: 206-211

Hasezawa, S., Sano, T. and Nagata, T. (1994) Oblique cell plate formation in tobacco BY-2 cells originates in double preprophase bands. J. Plant Res. 107: 355-359

Hasezawa, S., Kumagai, F. and Nagata, T. (1997) Sites of microtubule reorganization in tobacco BY-2 cells during cell-cycle progression. Protoplasma 198: 202-209

Hasezawa, S., Sano, T. and Nagata, T. (1998) The role of microfilaments in the organization and orientation of microtubles during the cell cycle transition from M phase to G_1 phase in tobacco BY-2 cells. Protoplasma 202: 105-114

Hasezawa, S., Ueda, K. and Kumagai, F. (2000) Time-sequence observations of microtubule dynamics throughout mitosis in living cell suspensions of stable transgenic *Arabidopsis* - direct evidence for the origin of cortical microtubules at M/G_1 Interface -. Plant Cell Physiol. 41: 244-250

Hazen, S.P., Scott-Craig, J.S. and Walton, J.D. (2002) Cellulose synthase-like genes of rice. Plant Physiol. 128: 336-340

Hepler, P.K. and Wolniak, S.M. (1984) Membranes in the mitotic apparatus: their structure

and function. Int. Rev. Cytol. 90: 169-238

Hoshino, H., Yoneda, A., Kumagai, F. and Hasezawa, S. (2003) Roles of actin-depleted zone and preprophase band in determining the division site of higher-plant cells, a tobacco BY-2 cell line expressing GFP-tubulin. Protoplasma 222: 157-165

Hush, J.M., Wadsworth, P., Callaham, D.A. and Hepler, P.K. (1994) Quantification of microtubule dynamics in living plant cells using fluorescence redistribusion after photobleaching. J. Cell Sci. 107: 775-784

Ishida, S., Takahashi, Y. and Nagata, T. (1993) Isolation of cDNA of an auxin-regulated gene encoding a G protein β subunit-like protein from tobacco BY-2 cells. Proc. Natl. Acad. Sci. U.S.A. 90: 11152-11156

Joshi, H.C. and Palevitz, B.A. (1996) γ-Tubulin and microtubule organization in plants. Trends Cell Biol. 6: 41-44

Kakimoto, T. and Shibaoka, H. (1987) Actin filaments and microtubules in the preprophase band and phragmoplast of tobacco cells. Protoplasma 140: 151-156

Kakimoto, T. and Shibaoka, H. (1988) Cytoskeletal ultrastructure of phragmoplast-nuclei complex isolated from cultured tobacco cells. Protoplasma (suppl) 2: 95-103

Kumagai, F., Hasezawa, S., Takahashi, Y. and Nagata, T. (1995) The involvement of protein synthesis Elongation Factor 1α in the organization of microtubules on the perinuclear region during the cell cycle transition from M phase to G_1 phase in tobacco BY-2 cells. Bot. Acta 108: 467-473

Kumagai, F. and Hasezawa, S. (2001) Dynamic organization of microtubules and microfilaments during cell cycle progression in higher plant cells. Plant Biol. 3: 4-16

Kumagai, F., Yoneda, A., Tomida, T., Sano, T., Nagata, T. and Hasezawa, S. (2001) Fate of nascent microtubules organized at the M/G_1 interface, as visualized by synchronized tobacco BY-2 cells stably expressing GFP-tubulin: Time-sequence observations of the reorganization of cortical microtubules in living plant cells. Plant Cell Physiol. 42: 723-732

Kumagai, F., Nagata, T., Yahara, N., Moriyama, Y., Horio, T., Naoi, K., Hashimoto, T.,

Murata, T. and Hasezawa, S. (2003) γ-Tubulin distribution during cortical microtubule reorganization at the M/G_1 interface in tobacco BY-2 cells. Eur. J. Cell Biol. 82: 43-51

Lee, Y.R.J., Giang, H.M. and Liu, B. (2001) A novel plant kinesin-related protein specifically associates with the phragmoplast organelles. Plant Cell 13: 2427

Linsmaier, E.M. and Skoog, F. (1965) Organic growth factor requirements of tobacco tissue cultures. Physiol. Plant. 18: 100-127

Liu, B., Joshi, H.C. and Palevitz, B.A. (1993) A γ-tubulin-related protein associated with the microtubule arrays of higher plants in a cell cycle-dependent manner. J. Cell Sci. 104: 1217-1228

Liu, B., Cyr, R.J. and Palevitz, B.A. (1996) A kinesin-like protein, KatAp, in the cells of Arabidopsis and other plants. Plant Cell 8: 119-132

Lloyd, C.W. (1987) The plant cytoskeleton: the impact of fluorescence microscopy. Annu. Rev. Plant Physiol. 38: 119-139

Ludin, B. and and Matus, A. (1998) GFP illuminates the cytoskeleton. Trends Cell Biol. 8: 72-77

Marc, J., Granger, C.L., Brincat, J., Fisher, D.D., Kao, T.H., McCubbin, A.G. and Cyr, R.J. (1998) A GFP-MAP4 reporter gene for visualizing cortical microtubule rearrangements in living epidermal cells. Plant Cell 10: 1927-1939

Mathur, J. and Chua, N.H. (2000) Microtubule stabilization leads to growth reorientation in Arabidopsis trichomes. Plant Cell 12: 465-477

Meier, I. (2001) The plant nuclear envelope. Cell Mol. Life Sci. 58: 1774-1780

Mineyuki, Y. and Palevitz, B.A. (1990) Relationship between preprophase band organization, F-actin and the division site in *Allium*. Fluorescence and morphometric studies on cytochalashin-treated cells. J. Cell Sci. 97: 283-295

Miyake, T., Hasezawa, S. and Nagata, T. (1997) Role of cytoskeleton components in the migration of nuclei during the cell cycle transition from G_1 phase to S phase of tobacco BY-2 cells. J. Plant Physiol. 150: 528-536

Mizuno, K. (1993) Microtubule-nucleation sites on nuclei of higher plant cells. Protoplasma

173: 77-85

Moore, R.C. and Cyr, R.J. (2000) Association between elongation factor-1α and microtubules in vivo is domain dependent and conditional. Cell Motil. Cytoskeleton 45: 279-292

Muller, I., Wagner, W., Volker, A., Schellmann, S., Nacry, P., Kuttner, F., Schwarz-Sommer, Z., Mayer, U. and Jurgens, G. (2003) Syntaxin specificity of cytokinesis in *Arabidopsis*. Nat. Cell Biol. 5: 531-534

Murata, T., Sonobe, S., Horio, T., Hori, K., Watanabe, Y. and Hasebe, M. (2004) Formation of cortical microtubules by branching from existing microtubules. Plant Cell Physiol. 45 (suppl.) : s115-s115

Nagai, T., Ibata, K., Park, E.S., Kubota, M., Mikoshiba, K. and Miyawaki, A. (2002) A variant of yellow fluorescent protein with fast and efficient maturation for cell-biological applications. Nat. Biotech. 20: 87-90

Nagata, T., Nemoto, Y. and Hasezawa, S. (1992) Tobacco BY-2 cell line as the "Hela" cell in the cell biology of higher plants. Int. Rev. Cytol. 132: 1-30

Nagata, T., Kumagai, F. and Hasezawa, S. (1994) The origin and organization of cortical microtubules during the transition between M and G_1 phase of the cell cycle as observed in highly synchronized cells of tobacco BY-2. Planta 193: 567-572

Nagata, T. and Kumagai, F. (1999) Plant cell biology through the window of the highly synchronized tobacco BY-2 cell line. Methods Cell Sci. 21: 123-127

Nishihama, R. and Machida, Y. (2001) Expansion of the phragmoplast during plant cytokinesis: a MAPK pathway may MAP it out. Curr. Opin. Plant Biol. 4: 507-512

Nishihama, R., Shoyano, T., Ishikawa, M., Araki, S., Tanaka, H., Asada, T., Irie, K., Ito, M., Terada, M., Banno, H., Yamazaki, Y. and Machida, Y. (2002) Expansion of the cell plate in plant cytokinesis requires a kinesin-like protein/MAPKKK complex. Cell 109: 87-99

Oka, M., Yanagawa, Y., Asada, T., Yoneda, A., Hasezawa, S., Sato, T. and Nakagawa, H. (2004) Inhibition of proteasome by MG-132 treatment causes extra phragmoplast formation and cortical microtubule disorganization during M/G_1 transition in synchronized tobacco cells. Plant Cell Physiol. 45: 1623-1632

Olyslaegers, G. and Verbelen, J.P. (1998) Improved staining of F-actin and co-localization of mitochondria in plant cells. J. Microsc. 192: 73-77

Palevitz, B.A. and Hepler, P.K. (1974) Control of plane of division during stomatal differentiation in *Allium*. II. Spindle reorientation. Chromosoma 46: 327-341

Pear, J.R., Kawagoe, Y., Schreckengost, W.E., Delmer, D.P. and Stalker, D.M. (1996) Higher plants contain homologs of the bacterial *celA* genes encoding the catalytic subunit of cellulose synthase. Proc. Natl. Acad. Sci. U.S.A. 93: 12637-12642

Saito, S., Watabe, S., Ozaki, H., Kobayashi, M., Suzuki, T., Kobayashi, H., Fusetani, N. and and Karaki, H. (1998) Actin-depolymerizing effect of dimeric macrolides, bistheonellide A and swinholide A. J. Biochem. 123: 571-578

Samuels, A.L., Giddings, T.H. and Staehelin, L.A. (1995) Cytokinesis in tobacco BY-2 and root tip cells: a new model of cell plate formation in higher plants. J. Cell Biol. 130: 1345-1357

Samuga, A. and Joshi, C.P. (2002) A new cellulose synthase gene (*PtrCesA2*) from aspen xylem is orthologous to Arabidopsis *AtCesA7* (irx3) gene associated with secondary cell wall synthesis. Gene 296: 37-44

Shimamura, M., Deguchi, H. and Mineyuki, Y. (1998) Meiotic cytokinetic apparatus in the formation of the linear spore tetrads of *Conocephalum japonicum* (Bryophyta). Planta 206: 604

Soyano, T., Nishihama, R., Morikiyo, K., Ishikawa, M. and Machida, Y. (2003) NQK1/NtMEK1 is a MAPKK that acts in the NPK1 MAPKKK-mediated MAPK cascade and is required for plant cytokinesis. Genes Dev. 17: 1055-1067

Spurr, A.R. (1969) A low viscosity epoxy resin embedded medium for electron microscopy. J. Ultrastruct. Res. 26: 31-42

Staiger, C.J. and Lloyd, C.W. (1991) The plant cytoskeleton. Curr. Opin. Cell Biol. 3: 33-42

Stoppin, V., Vantard, M., Schmit, A.C. and Lambert, A.M. (1994) Isolated plant nuclei nucleate microtubule assembly: The nuclear surface in higher plants has centrosome-like activity. Plant Cell 6: 1099-1106

Stoppin, V., Lambert, A.M. and Vantard, M. (1996) Plant microtubule-associated proteins (MAPs) affect microtubule nucleation and growth at plant nuclei and mammalian centrosomes. Eur. J. Cell Biol. 69: 11-23

Ueda, K., Matsuyama, T. and Hashimoto, T. (1999) Visualization of microtubules in living cells of transgenic *Arabidopsis thaliana*. Protoplasma 206: 201-206

Ueda, K. and Matsuyama, T. (2000) Rearrangement of cortical microtubules from transverse to oblique or longitudinal in living cells of transgenic *Arabidopsis thaliana*. Protoplasma 213: 28-38

Valster, A.H. and Hepler, P.K. (1997) Caffeine inhibition of cytokinesis: effect on the phragmoplast cytoskeleton in living *Tradescantia* samen hair cells. Protoplasma 196: 155-166

Vantard, M., Levilliers, N., Hill, A.M., Adoutte, A. and Lambert, A.M. (1990) Incorporation of *Paramecium* axonemal tubulin into higher plant cells reveals functional sites of microtubule assembly. Proc. Natl. Acad. Sci. U.S.A. 87: 8825-8829

Verma, D.P.S. (2001) Cytokinesis and building of the cell plate in plants. Annu. Rev. Plant Physiol. Plant Mol. Biol. 52: 751-784

Völker, A., Stierhof, Y.-D. and Jürgens, G. (2001) Cell cycle-independent expression of the *Arabidopsis* cytokinesis-specific syntaxin KNOLLE results in mistargeting to the plasma membrane and is not sufficient for cytokinesis. J. Cell Sci. 114: 3001-3012

Waizenegger, I., Lukowitz, W., Assaad, F., Schwarz, H., Jurgens, G. and Mayer, U. (2000) The *Arabidopsis KNOLLE* and *KEULE* genes interact to promote vesicle fusion during cytokinesis. Curr. Biol. 10: 1371-1374

Wasteneys, G.O., Gunning, E.S. and Hepler, P.K. (1993) Microinjection of fluorescent brain tubulin reveals dynamic properties of cortical microtubules in living plant cells. Cell Motil. Cytoskeleton 24: 205-213

Wymer, C.L., Shaw, P.J., Warn, R.M. and Lloyd, C.W. (1997) Microinjection of fluorescent tubulin into plant cells provides a representative picture of the cortical microtubule array. Plant J. 12: 229-234

Yanagawa, Y., Hasezawa, S., Kumagai, F., Oka, M., Fujimuro, M., Naito, T., Makino, T., Yokosawa, H., Tanaka, K., Komamine, A., Hashimoto, J., Sato, T. and Nakagawa, H. (2002) Cell-cycle dependent dynamic change of 26S proteasome distruction in tobacco BY-2 cells. Plant Cell Physiol. 43: 604-613

Yoneda, A. and Hasezawa, S. (2003) Origin of cortical microtubules organized at M/G_1 interface: recruitment of tubulin from phragmoplast to nascent microtubules. Eur. J. Cell Biol. 82:461-71

Yoneda, A., Kutsuna, N. and Hasezawa, S. (2003) Dynamic organization of microtubules and vacuoles visualized by GFP in living plant cells. Recent Res. Dev. Plant Mol. Biol. 1: 127-137

Yoneda, A., Akatsuka, M., Kumagai, F. and Hasezawa, S. (2004) Disruption of actin microfilaments causes cortical microtubule disorganization and extra-phragmoplast formation at M/G_1 interface in synchronized tobacco cells. Plant Cell Physiol. 45: 761-769

Yoneda, A., Akatsuka, M., Hoshino H., Kumagai, F. and Hasezawa, S. (2005) Decision of spindle poles and division plane by double preprophase bands in a BY-2 cell line expressing GFP-tubulin. Plant Cell Physiol. in press

Yuan, M., Shaw, P.J., Warn, R.M. and Lloyd, C.W. (1994) Dynamic reorientation of cortical microtubules, from transverse to longitudinal, in living plant cells. Proc. Natl. Acad. Sci. U.S.A. 91: 6050-6053

Zhang, D., Wadsworth, P. and Hepler, P.K. (1990) Microtubule dynamics in living dividing plant cells: Confocal imaging of microinjected fluorescent brain tubulin. Proc. Natl. Acad. Sci. U.S.A. 87: 8820-8824

Zhong, R., Morrison, I.I.I. H., Freshour, G.D., Hahn, M.G. and Ye, Z.-H. (2003) Expression of a mutant from of cellulose synthase AtCesA7 causes dominant negative effect on cellulose biosynthesis. Plant Physiol. 132: 786-795